

Unified Capacity Limit of Non-Coherent Wideband Fading Channels

Felipe Gómez-Cuba*, *Student Member, IEEE*, Jinfeng Du*, *Member, IEEE*,
Muriel Médard, *Fellow, IEEE*, and Elza Erkip, *Fellow, IEEE*

Abstract

In non-coherent wideband fading channels where energy rather than spectrum is the limiting resource, peaky and non-peaky signaling schemes have long been considered species apart, as the first approaches asymptotically the capacity of a wideband AWGN channel with the same average SNR, whereas the second reaches a peak rate at some finite *critical bandwidth* and then falls to zero as bandwidth grows to infinity. In this paper it is shown that this distinction is in fact an artifact of the limited attention paid in the past to the product between the bandwidth and the fraction of time it is in use. This fundamental quantity, called *bandwidth occupancy*, measures average bandwidth usage over time. For all signaling schemes with the same bandwidth occupancy, achievable rates approach to the wideband AWGN capacity within the same gap as the bandwidth occupancy approaches its critical value, and decrease to zero as the occupancy goes to infinity. This unified analysis produces quantitative closed-form expressions for the ideal bandwidth occupancy, recovers the existing capacity results for (non-)peaky signaling schemes, and unveils a trade-off between the accuracy of approximating capacity with a generalized Taylor polynomial and the accuracy with which the optimal bandwidth occupancy can be bounded.

This work was presented in part at IEEE International Symposium on Information Theory, Hong Kong, July 2015 [1].

This work is supported in part by the MIT Wireless Center, the National Science Foundation under Grant 1302336, the NYU WIRELESS, and the Swedish Research Council (VR) under Grant 637-2013-473. This work is also funded by FPU12/01319 MECD, University of Vigo and Xunta de Galicia, Spain.

F. Gómez-Cuba is with AtlantTIC, University of Vigo, C.P. 36310 Vigo, Spain (Email: fgomez@gti.uvigo.es).

J. Du is with Nokia Bell Labs, Holmdel, NJ 07733, USA. He was with Massachusetts Institute of Technology, Cambridge, MA, USA (Email: jinfeng.du@bell-labs.com).

M. Médard is with Massachusetts Institute of Technology, Cambridge, MA 02139, USA (Email: medard@mit.edu).

E. Erkip is with NYU Tandon School of Engineering, Brooklyn, NY 11201, USA (Email: elza@nyu.edu).

*The first two authors contributed equally to this work.

Index Terms

Wideband regime, peaky signals, non-peaky signals, bandwidth occupancy

I. INTRODUCTION AND RELATED WORK

Recently there has been great interest in wireless channels with a large bandwidth, owing in part to the prospective investments onto the millimeter wave bands, where vast quantities of new spectrum is readily available [2]–[5]. In a frequency selective fading channel where there is no channel state information at the receiver (CSIR) or the transmitter, the wideband capacity is affected by the growing uncertainty in the channel impulse response. As bandwidth grows while energy is constrained, it becomes infeasible to estimate the channel coefficients to a precision sufficient for coherent detection. Moreover, if the transmitted signal power is spread across all the available bandwidth and time slots, the desired signal would be buried by the channel uncertainty when bandwidth is too large. Médard and Gallager proved this [6] through an upper bound to the rate that is proportional to the ratio between the fourth moment of the signal ($E[|x|^4]$) and its bandwidth (B), i.e., $R < \propto E[|x|^4]/B$. That is, to achieve rates above zero when $B \rightarrow \infty$, one has to make $E[|x|^4]$ grow at least as fast as B by concentrating the power of the signal in a vanishing fraction of its transmitted symbols (i.e. infrequent bursts of very large power).

In this paper we investigate the capacity bounds of non-coherent wideband fading channels in multi-input multi-output (MIMO) setup where both the signaling bandwidth and signal peakiness are design parameters. The channel is assumed to be rich scattering, frequency selective, block fading with a coherence time T_c and a delay spread D , such that the channel frequency response becomes uncorrelated for frequencies apart from more than one coherence bandwidth $B_c \triangleq 1/D$. The channel coherence length, $B_c T_c$, is assumed to be large for capacity analysis purposes, as in almost all practical channels, $B_c T_c \gg 1$. In our expressions we temporarily treat $B_c T_c$ as a fixed parameter to derive closed-form expressions, where approximation errors originated from $B_c T_c \gg 1$ are highlighted in small- o expressions parametrized by higher order terms of $B_c T_c$. We further assume that $B_c T_c > N_t$, which is easily satisfied in typical systems where the number of transmit antennas is not massive. We generalize the analysis method in [7], developed for non-peaky signaling in single-input single-output (SISO) systems, to MIMO systems and extend it to arbitrary level of signal peakiness by enforcing a transmission duty cycle $\delta \in (0, 1]$. The duty

cycle prescribes a bursty transmission scheme where the transmitter is active only for a fraction δ of time with boosted signal power P/δ harnessed from the $(1-\delta)$ silent-cycle. Denoting by $C(B)$ the capacity of the unconstrained non-coherent channel and by $C(B, \delta)$ the maximal rate achieved by using bandwidth B and duty cycle δ , for all $B > 0$ and $\delta \in (0, 1]$, we have

$$C(B, \delta) < C(B) \leq C^\infty \triangleq N_r P / N_0 \text{ [nats/s]},$$

where C^∞ is the limit capacity of the coherent channel at infinite bandwidth, P is the received signal power, N_0 is the noise power spectral density, and N_r is the number of receive antennas. Note that the first inequality is strict because we do not exploit the position of the active symbols to convey information. We show in Sec. III that $C(B, \delta)$ is upper and lower bounded by

$$R^{\text{LB}}(\delta B) \leq C(B, \delta) \leq R^{\text{UB}}(\delta B).$$

Note that both the upper and lower bounds, up to a small approximation error $o(1/\delta B)$, depend on B and δ only through the product δB , which measures average bandwidth usage over time and is named the “bandwidth occupancy”. Our results show that for a series of signaling schemes with finite signaling bandwidth B larger or equal to a *critical bandwidth occupancy* $(\delta B)_{\text{crit}}$, which falls in a range prescribed by closed-form expressions, it is possible to achieve rates close to C^∞ within the same rate penalty

$$C(B, \delta) \geq N_r \frac{P}{N_0} - \Delta_C, \quad \Delta_C = N_r \frac{P}{N_0} \sqrt{\frac{1 + \log B_c T_c}{B_c T_c} (\kappa - 2 + N_t + N_r) \log \pi}, \quad (1)$$

as long as the duty cycle is $\delta = \frac{(\delta B)_{\text{crit}}}{B}$. Here N_t is the number of transmit antennas and $\kappa > 0$ is the kurtosis (whose definition is deferred to Sec. II) of the channel. Thus, it is possible to approach C^∞ up to the same gap with any $\delta \in (0, 1]$. Note also that $B_c T_c \gg 1$ leads to $\Delta_C \simeq 0$ and $R(\delta B^{\text{crit}}) \simeq C^\infty$. Furthermore, we show in Sec. IV that the analysis of $C(B)$ with peaky signaling in literature [8], [9] experiences exactly this same gap to C^∞ , although we obtained (1) using non-peaky signals [7] and a power-boosting duty cycle $\delta \in (0, 1]$. Fig. 1 illustrates the relation between our bounds $C(B, \delta)$, capacity $C(B)$, and the coherent wideband channel limit C^∞ .

The main contribution of this paper is the unified approximation of C^∞ with peaky and non-peaky signaling, showing that these two extremes can be connected by all level of peakiness parametrized by the duty cycle $\delta \in (0, 1]$. All signaling schemes (B, δ) with the same bandwidth occupancy $\delta B = (\delta B)_{\text{crit}}$ approach C^∞ within the same capacity gap up to a small approximation

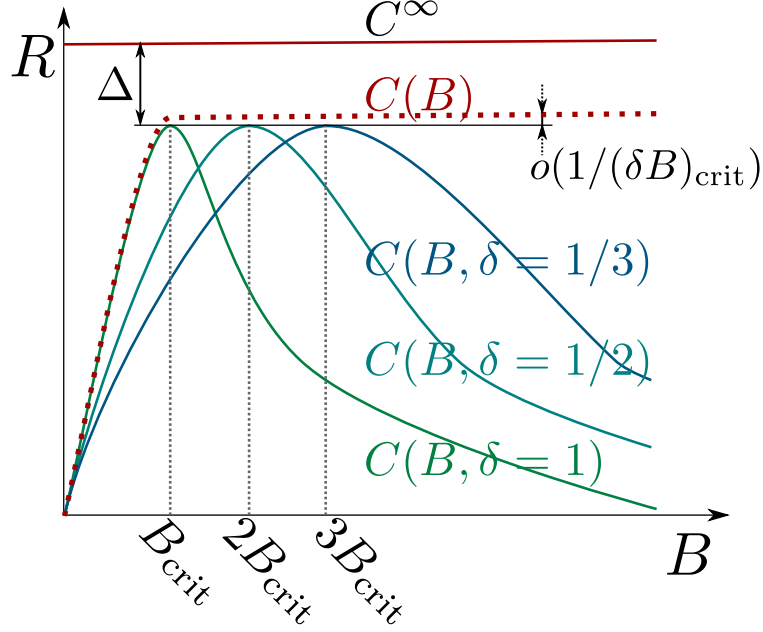


Figure 1. All transmission strategies with the same bandwidth occupancy $\delta B = (\delta B)_{\text{crit}}$ achieve the same polynomial approximation of C^∞ at different bandwidths. $C(B)$ is separated from the maximum $C(B, \delta)$ by a difference of $o(1/(\delta B)_{\text{crit}})$.

error of $o(1/(\delta B)_{\text{crit}})$. We have also derived closed-form expressions for capacity bounds and critical bandwidth occupancy for all values $\delta \in (0, 1]$, which provide valuable engineering insights and tools to quantify the resources needed to approach C^∞ . As a byproduct, we obtained a group of closed-form bounds to the range of $(\delta B)_{\text{crit}}$ that are implicit in the existing literature [8], [9]. These parametric bounds can be tuned based on an *accuracy-resolution tradeoff* to complement the range identified in our non-peaky signaling analysis.

A. Related Work

The results in [6] have been extended to signals with output fourth-order constraint [10] or small input peakiness constraint [11]. Telatar and Tse [12] related channel uncertainty to the number of resolvable independent paths, and showed that in a rich scattering environment where this number increases with B , the rate can grow as long as the signal power in each path is not too low, but it starts decreasing when the number of paths is above a critical value.

The capacity of a wideband fading channel achieves *first order optimality* if, as B goes to infinity, it has the same limit as a wideband additive white Gaussian noise (AWGN) channel.

This has been studied in [8], [9], [12]–[14] and the linear in power capacity limit for MIMO is

$$\lim_{B \rightarrow \infty} C(B)^{\text{noncoherent}} = \lim_{B \rightarrow \infty} C(B)^{\text{AWGN}} = \frac{N_r P}{N_0}.$$

To quantify the “exchange rate” of bandwidth to capacity in the asymptotic regime where $B \rightarrow \infty$, the concept of *wideband slope* was introduced in [13]. A larger wideband slope means that higher rate gain is obtained given the same amount of extra bandwidth. The wideband slope is studied in [13, Theorem 9] based on the second order term of a Taylor series expansion of the spectral efficiency (C/B , in nats/s/Hz) with respect to the signal-to-noise ratio (SNR) at each receive antenna, $\text{SNR} \triangleq P/(BN_0)$. The wideband slope is inversely proportional to the second order derivative of the spectral efficiency at $\text{SNR}=0$, which is finite for AWGN and coherent fading channels (i.e., with perfect CSIR) but $-\infty$ for non-coherent scenarios (i.e., with no CSIR). Thus the coherent fading channel is *second order optimal* but the non-coherent channel is not. This abrupt distinction contrasts with the intuition that, as the channel coherence time T_c and/or frequency B_c grow, channel estimation becomes increasingly rewarding and the capacity of the non-coherent channel converges to the capacity of the coherent channel. This contradiction was resolved in [8], [9] by showing that in non-coherent Rayleigh fading channels the spectral efficiency $C(B)/B$ is better represented by a generalized Taylor polynomial of order $1+\alpha < 2$,

$$\frac{C(B)}{B} = N_r \left(\frac{P}{N_0 B} \right) - \frac{N_r(N_r + N_t)}{2N_t} \left(\frac{P}{N_0 B} \right)^{1+\alpha} + o\left(\frac{1}{B^{1+\alpha}}\right), [\text{nats/s/Hz}], \quad (2)$$

where the exponent $\alpha \in (0, 1)$ grows with increasing $B_c T_c$. The first term equals C^∞/B , representing a *first order optimal* upper bound of the spectral efficiency when rate is power-limited. The third term captures the approximation error, that vanishes faster than $B^{-(1+\alpha)}$ as $B \rightarrow \infty$. The second term represents the penalty from lack of channel knowledge. It contains $\text{SNR}^{1+\alpha}$, a sub-quadratic term ($1+\alpha < 2$) that characterizes the convergence speed of the spectral efficiency for non-coherent fading channels. Representing (2) by the second order Taylor polynomial leads to an infinite coefficient to the term SNR^2 (wideband slope) and lack of second order optimality as in [13]. In this paper the word “polynomial” refers to these generalized Taylor polynomials with real-valued exponents.

Although peaky signals are imperative to achieve first order optimality [13, Th. 7], they are challenging to synthesize owing to hardware non-linearity and the infinite amount of bandwidth they require in non-coherent channels. If a small gap from C^∞ at a large but finite bandwidth is

admissible, which is the case in all practical applications of asymptotic results, recent works have shown that non-peaky signals may suffice. For example, Zhang and Laneman [15] investigated the achievable rate of phase-shift keying (PSK) for frequency-flat time-varying non-coherent Rayleigh fading channels. Under average power constraints, this signaling scheme approaches the wideband capacity limit for low but not too low SNRs. For signals subject to both peak and average power constraints, it was observed in [16] that the gap between capacity upper and lower bounds can be very small for discrete-time frequency-flat Rayleigh fading channels. The capacity of non-coherent time-frequency selective wide-sense stationary uncorrelated scattering (WSSUS) channels with both peak and average power constraints has been studied in [17], where bell-shaped capacity upper and lower bounds were established and the capacity optimal bandwidth, the *critical bandwidth*, was coarsely identified as a function of the peak power and the scattering function. For flat scattering functions, the capacity bounds depend on the system bandwidth and the input-signal peak constraint only through their ratio. The results in [17] have been extended to MIMO in [18], where the impact of transmitter/receiver antenna correlation on capacity was also investigated. Lozano and Porrat [7] considered non-peaky signaling in SISO systems under a general fading distribution. Their results show that, when bandwidth is not too large, there is a transitory first stage where rate $R(B)$ grows with B before approaching a maximum $R(B_{\text{crit}})$ at the critical bandwidth $B=B_{\text{crit}}$, beyond which the rate $R(B)$ decreases to zero as B grows unbounded. By resorting to computation of mutual information rather than the capacity analysis as in [17], [18], they provided closed-form expressions to the maximum rate and the corresponding capacity gap,

$$R(B_{\text{crit}}) = \frac{P}{N_0} - \Delta, \quad \Delta = \frac{P}{N_0} \sqrt{\frac{1 + \log B_c T_c}{B_c T_c} \kappa \log \pi}, \quad (3)$$

where Δ vanishes with increasing coherence length $B_c T_c$. For Rayleigh fading, closed-form expressions for the range of B_{crit} were also derived.

Even though [13, Th. 7] found that peaky signaling is imperative to achieve first order optimality, the definition of first order optimality enforces an implicit requirement to make bandwidth grow as high as possible ($B \rightarrow \infty$). Thus, only those inputs that approach C^∞ when B is infinite are covered by [13, Th. 7]. What our results show is that C^∞ can be approached as well using a finite bandwidth B and non-peaky signaling.

Unlike in [8], [9] where the non-coherent wideband fading channel capacity $C(B)$ is obtained

by using the position of signal pulses in the frequency domain (i.e., FSK) to convey information, in our analysis the position of actively transmitted symbols in the time domain, which collectively defines the active-cycle, is revealed in advance to the receiver and therefore bears no information.

Our capacity bounds are based on computation of mutual information with constrained input signal peakiness – in the sense of kurtosis – that is controlled by enforcing a duty cycle $\delta \in (0, 1]$. This is in contrast to [17], [18] where capacity analysis is used with peak constraint on the amplitude of transmitting signals. Our choice of mutual information analysis can be justified from two aspects: even though we do not design inputs to achieve the capacity bounds we can guarantee such inputs exist as long as the channel and noise are stationary weakly mixing processes, see [19, Prop. 2.1]; the rate upper and lower bounds and the range of the critical bandwidth occupancy can be described in closed-form expressions, which are otherwise difficult to obtain using capacity analysis, see [17], [18].

Our choice of using duty cycle rather than peak constraint on signal amplitude [16], [17] to control the signal peakiness can be justified as follows: given the same average power constraint, a peak constraint on signal amplitude will limit the peak-to-average power ratio (PAPR), which is sufficient but not necessary to generate a constraint on signal peakiness. Signals with finite peakiness may have infinite PAPR (e.g., Gaussian signal has infinite PAPR but only a small kurtosis $\kappa=2$). It must be noted that in non-coherent wideband fading channels, capacity is related to the peakiness in the kurtosis sense [6], [13].

The rest of this paper is organized as follows. We introduce the system model in Sec. II and present our unified analysis of wideband non-coherent channel in Sec. III. We describe our non-coherent polynomial approximation to coherent capacity, and discuss its relation with literature in Sec. IV. Finally our conclusions are in Sec. V.

II. SYSTEM MODEL

We consider a rich scattering, frequency selective, block fading, $N_t \times N_r$ MIMO wideband channel with an impulse response $h(t)^{(u,v)}$ between antennas (u, v) . For compactness we assume that all channels experience a coherence time T_c and a delay spread D and the channel frequency response becomes uncorrelated for frequencies apart more than one coherence bandwidth $B_c \triangleq 1/D$. We focus only on the frequency signaling scheme since it is known [7] that differences between frequency and time signaling only affect the scaling with bandwidth in its vanishing

higher order terms. In the following we present the characteristics of the discrete-time system model¹. Justification of our choice of the wideband fading model is presented in Appendix A.

Our model starts from a continuous-time wideband fading channel, followed by the discretization/sampling process on the input-output signals. This provides a signaling scheme where every T_c seconds, the transmitted signal $x^{(u)}[n]$ with bandwidth B carries $K=BT_c$ complex samples on antenna $u \in [0, N_t-1]$. Taking a K -point DFT of the complex samples for each antenna and then stacking all the N_t vectors up, the transmitted codeword is uniquely defined by the $N_t K \times 1$ vector \mathbf{x} that satisfies the average power constraint

$$\frac{1}{K} \mathbb{E} [|\mathbf{x}|^2] \leq P T_c.$$

For $i=kN_t+u$, the i -th coefficient of \mathbf{x} , denoted as $x^{(i)}$, corresponds to the transmitted signal on antenna u with DFT index $k \in \{0, 1, \dots, K-1\}$. For each pair of antennas (u, v) , the discrete samples of the channel have $M=BD$ i.i.d. coefficients $h^{(u,v)}[n]$, $n=0, 1, \dots, M-1$, with $M/K=D/T_c=\frac{1}{B_c T_c}$. After applying K -point DFT to each discrete channel sequence $h^{(u,v)}[n]$, we define a block-diagonal matrix

$$\mathbf{H} = \left(\begin{array}{c|c|c|c} \mathbf{H}[0] & \mathbf{0} & \dots & \mathbf{0} \\ \hline \mathbf{0} & \mathbf{H}[1] & \ddots & \vdots \\ \hline \vdots & \ddots & \ddots & \mathbf{0} \\ \hline \mathbf{0} & \dots & \mathbf{0} & \mathbf{H}[K-1] \end{array} \right), \quad (4)$$

where $\mathbf{H}[k]$ contains in its (v, u) -th element the k -th DFT coefficient of $h^{(u,v)}[n]$, whose distribution is determined by the impulse response $h(t)^{(u,v)}$. Each channel only has M i.i.d. coefficients and any two blocks $\mathbf{H}[k]$ and $\mathbf{H}[k']$ are correlated only if $|k-k'| < B_c T_c$. We also define the average gain of the n -th channel coefficient $g_n^{(u,v)} = \mathbb{E} [|h^{(u,v)}[n]|^2]$ satisfying $\sum_{n=0}^{M-1} g_n^{(u,v)} = 1$.

When $D \ll T_c$, a cyclic prefix with negligible influence in rate can be inserted to remove the inter-symbol interference and the signal received on each fading realization, T_c , depends only on the state of the channel and signal transmitted during the same realization. After applying K -point DFT to the received signal, we can represent the system as

$$\mathbf{y} = \mathbf{H}\mathbf{x} + \mathbf{z}, \quad (5)$$

¹The equivalence between the discrete-time and continuous-time channel models for SISO is established in [20] using sampling and DFT, and in [21] using pulse shaping filter banks with Weyl-Heisenberg projection. Our result uses MIMO in a rich scattering environment and we provide explicit mapping of the channel coefficients between two different discrete-time models.

where \mathbf{y} is a $N_r K \times 1$ vector whose i -th element $y^{(i)}$, with $i = kN_r + v$, corresponds to the signal received on antenna v with DFT coefficient index k . The noise vector \mathbf{z} follows a Gaussian distribution with PSD N_0 ($\mathcal{CN}(0, \mathbf{I}_{N_r K} N_0 T_c)$).

Some references, such as [8], [9], use a different discrete-time model with fewer frequency bins, each experiencing an independent fading coefficient that repeats itself for many consecutive symbols. We prove in Appendix B that the two discrete-time models are compatible. In Appendix C we show that the two models are equivalent at the continuous-time level using concepts of multi-carrier modulations and we provide explicit mapping of the channel coefficients between the two models. Therefore our results are independent of the model chosen.

Wideband capacity is related to peakiness in the sense of the normalized fourth moment of the inputs, or *kurtosis* [6], [13]. Given a stochastic sequence $A(t)$, its kurtosis is defined as

$$\kappa(A(t)) \triangleq \frac{\mathbb{E}_{A(t)} [|a(t)|^4]}{\mathbb{E}_{A(t)} [|a(t)|^2]^2}, \quad (6)$$

where the time index (t) may be dropped if the process is stationary. By enforcing a duty cycle $\delta \in (0, 1]$ on the input signal \mathbf{x} , the system is converted into the time-alternation of an active stage for a fraction δ of the time with boosted power $P' = \frac{P}{\delta}$, and an idle stage for a fraction $(1-\delta)$ of the time. Let $\tilde{\mathbf{x}}$ be a non-peaky signal with power P and finite kurtosis $\kappa(\tilde{\mathbf{x}})$. We introduce a binary random variable $c \in \{0, 1\}$ to represent the use of each fading block of size $T_c \times B_c$, where $c=1$ means the channel block is active for signal transmission and $c=0$ means idle, with probability $P_r(c=1) = \delta$. We reveal c to the receiver in advance, which will reduce the rate as

$$C(B, \delta) = \mathbb{I}(\mathbf{x}; \mathbf{y}|c) = \mathbb{I}(\mathbf{x}, c; \mathbf{y}) - \mathbb{I}(c; \mathbf{y}) = \mathbb{I}(\mathbf{x}; \mathbf{y}) - \mathbb{I}(c; \mathbf{y}) \leq \mathbb{I}(\mathbf{x}; \mathbf{y}),$$

where $0 \leq \mathbb{I}(c; \mathbf{y}) \leq H(c)$ with all equalities hold for $\delta=1$. The duty cycle induces a new signal

$$\mathbf{x} = \tilde{\mathbf{x}} \sqrt{\frac{c}{\mathbb{E}[c]}} = \begin{cases} \tilde{\mathbf{x}}/\sqrt{\delta}, & \text{w.p. } \delta, \\ 0, & \text{w.p. } 1-\delta, \end{cases} \quad \text{with } \kappa(\mathbf{x}) = \frac{\mathbb{E}[|\mathbf{x}|^4]}{\mathbb{E}[|\mathbf{x}|^2]^2} = \frac{\mathbb{E}[|\tilde{\mathbf{x}}|^4]}{\delta \mathbb{E}[|\tilde{\mathbf{x}}|^2]^2} = \frac{\kappa(\tilde{\mathbf{x}})}{\delta}. \quad (7)$$

Therefore we can effectively adjust the peakiness (in the sense of kurtosis) of signaling without imposing any extra constraint on the distribution of the active signal $\tilde{\mathbf{x}}$.

III. BANDWIDTH OCCUPANCY LIMIT

Our analysis is a generalization of the the SISO analysis with non-peaky signaling in [7]. We extend the process to MIMO systems and to an arbitrary level of signaling peakiness through the tunable duty cycle parameter $\delta \in (0, 1]$. Both analyses follow four steps, represented in Fig. 2.

- 1) Find a bell-shaped lower bound $R^{LB}(\delta B) \leq C(B, \delta)$;
- 2) Determine the unique maximum of $R^{LB}(\delta B)$, $R^{LB}((\delta B)^*)$;
- 3) Find a bell-shaped upper bound $R^{UB}(\delta B) \geq C(B, \delta)$;
- 4) Determine $(\delta B)^+$ and $(\delta B)^-$ such that $R^{UB}((\delta B)^+) = R^{UB}((\delta B)^-) = R^{LB}((\delta B)^*)$.

The result of [7] shows that the capacity of a non-coherent fading channel with non-peaky signaling ($\delta=1$, finite κ) grows with bandwidth B only when it is below a *critical bandwidth* B_{crit} , which falls into the range $[B^-, B^+]$. A system operating with insufficient bandwidth $B < B_{\text{crit}}$ is less efficient in converting available signal energy into rate due to the sub-linear law between rate and SNR, and the corresponding achievable rate grows with increasing bandwidth. When signal power spreads over too much bandwidth $B > B_{\text{crit}}$, the channel-uncertainty induced penalty grows with increasing bandwidth and the achievable rate decreases to zero as $B \rightarrow \infty$. Therefore, contrary to the wideband AWGN channel where “the deeper into the low-SNR regime, the better”, in the non-coherent fading channel the guideline is “enter, but not in excess, in the low-SNR regime”, with the optimal operation point at B_{crit} . Our result shows that for any $B > B_{\text{crit}}$ it is possible to bring the capacity back to the same optimal value, up to a small approximation error of order $o(1/B_{\text{crit}})$, by imposing a duty-cycle parameter $\delta = (\delta B)_{\text{crit}}/B$ and a power-boost $P' = P/\delta$ on the original non-peaky signaling. Moreover, in Sec. IV we show that this strategy achieves the same gap from C^∞ as in the peaky-signaling analysis [8], [9].

A. Capacity Lower Bound for $C(B, \delta)$

As in [7], our lower bound is obtained by first calculating the maximum achievable rate of a coherent non-peaky signaling under the average power constraint and then deducting the maximum rate penalty from lack of CSI. Therefore it is valid for general channel fading distributions and for any value of B and $B_c T_c > N_t$. The potential spatial correlation among different antennas is not considered here.

Lemma 1. *The achievable rate in a wideband non-coherent channel with i.i.d. fading and a duty cycle $\delta \in (0, 1]$ is lower bounded by*

$$R^{LB}(\delta B) = \frac{P N_r}{N_0} \left[1 - \frac{P(\kappa - 2 + N_t + N_r)}{2\delta B N_t N_0} \right] - \frac{\delta B N_t N_r}{B_c T_c} \log \left(1 + \frac{P}{\delta B N_t N_0} B_c T_c \right), \quad (8)$$

where $\kappa = \kappa(h)$ is the kurtosis of the channel fading coefficients.

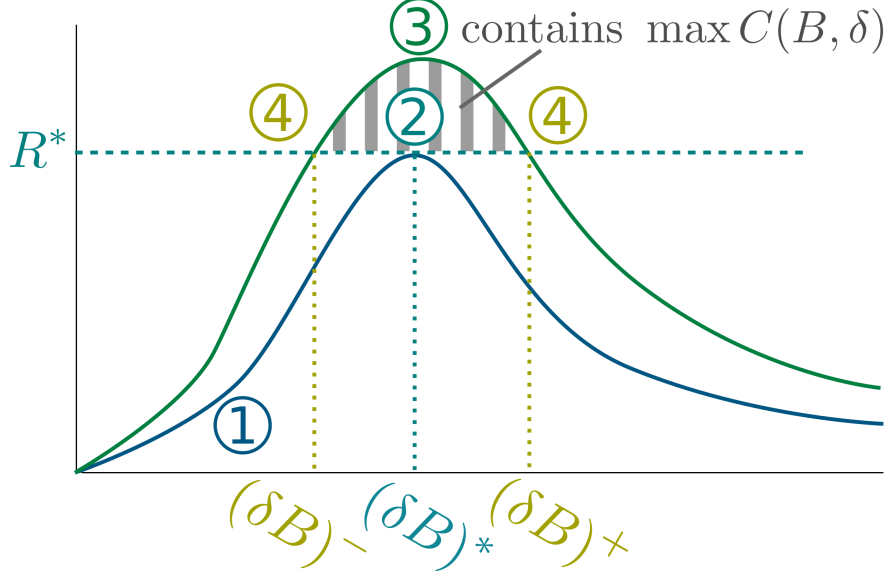


Figure 2. Our four-step analysis of critical bandwidth occupancy. Substituting (δB) by B gives the original analysis by [7].

Proof: See Appendix D. ■

The *kurtosis* κ for many fading distributions are in the range of $[1, 2]$. For example, as given in [7], $\kappa = 2$ for Rayleigh fading, $\kappa = 2 - 4k^2/(1+2k)^2$ for Rice fading with factor $k > 0$, and $\kappa = 1 + 1/m$ for Nakagami- m fading channels.

Remark 1. Even though the duty-cycle constrained capacity $C(B, \delta)$ might be two-dimensional function of δ and B , the lower bound is only a function of the product δB .

B. Maximum of R^{LB}

We use the assumption that $B_c T_c \gg 1$ to determine the maximum of the capacity lower bound R^{LB} . For any finite $B_c T_c$ we can approximate the optimal $(\delta B)^*$ and the associated maximum rate up to an error term $o\left(\sqrt{\frac{\log(B_c T_c)}{B_c T_c}}\right)$ that decreases to zero as $B_c T_c \rightarrow \infty$.

Lemma 2. $R^{LB}(\delta B)$ is maximized at $\delta B = (\delta B)^*$ with

$$(\delta B)^* = \frac{P}{N_0 N_t} \sqrt{\frac{B_c T_c}{\log(B_c T_c)} (\kappa - 2 + N_t + N_r)} + o\left(\sqrt{\frac{B_c T_c}{\log(B_c T_c)}}\right), \quad (9)$$

$$R^{LB}((\delta B)^*) \geq \frac{P N_r}{N_0} \left[1 - \sqrt{\frac{1 + \log(B_c T_c)}{B_c T_c} (\kappa - 2 + N_t + N_r) \log \pi} \right] - o\left(\sqrt{\frac{\log(B_c T_c)}{B_c T_c}}\right). \quad (10)$$

Proof: See Appendix E. ■

Remark 2. We would like to emphasize that the rate-maximizing bandwidth occupancy $(\delta B)^*$ is very large given the fact that the channel coherence $B_c T_c$ usually ranges from a few hundreds to hundreds of thousands. For example, assuming 2×2 MIMO over Rayleigh fading ($\kappa=2$) with $P/N_0=70$ dB, we have $(\delta B)^* \simeq 120$ MHz with capacity gap $\Delta/C^\infty < 0.18$ for $B_c T_c = 10^3$, and $(\delta B)^* \simeq 930$ MHz with $\Delta/C^\infty < 0.03$ for $B_c T_c = 10^5$.

C. Capacity Upper Bound for $C(B, \delta)$

We obtain a capacity upper bound for the case when channel is Rayleigh distributed. The bound, up to an error term of $o(1/\delta B)$ that vanishes as $\delta B \rightarrow \infty$, applies to any value of B and $B_c T_c > N_t$ and all inputs subject to constraints of average power P and signaling duty cycle δ .

Lemma 3. The achievable rate of signaling schemes with duty cycle $\delta \in (0, 1]$ in a wideband non-coherent Rayleigh fading channel is upper bounded by

$$R^{UB}(\delta B) = \frac{P N_r}{N_0} \left[1 - \frac{P}{2\delta B N_0} - \frac{\delta B N_t N_0}{P B_c T_c} \mathbb{E}_\psi \left[\log \left(1 + \frac{P}{\delta N_t B N_0} B_c T_c g_{\min} \psi \right) \right] \right] + o\left(\frac{1}{\delta B}\right), \quad (11)$$

where $g_{\min} = \min_{m,u,v} \mathbb{E} [|h^{(u,v)}[m]|^2]$ is the minimum non-zero square channel gain among all delays and antenna pairs, and the random variable ψ is defined as

$$\psi = \arg \min_{\psi_{K,n}} \mathbb{E} \left[\log \left(1 + \frac{P g_{\min} \psi_{K,n}}{\delta N_t N_0 B} B_c T_c \right) \right], \quad \text{where } \psi_{K,n} \triangleq \frac{1}{K} \left| \sum_{k=0}^{K-1} \frac{\mathbf{x}_k}{\sqrt{P}} e^{-j2\pi \frac{kn}{MN_t}} \right|^2. \quad (12)$$

Proof: See Appendix F. ■

Remark 3. The auxiliary variable ψ is bounded ($\psi > 0$, $\mathbb{E}[\psi] \leq 1$) and serves here as a placeholder for the minimization of the last term of the bound, which is implicitly determined by (12).

D. Critical Bandwidth Occupancy

We obtain the range of values of δB where the upper bound is larger than $R^{LB}((\delta B)^*)$. $C(B, \delta)$ can approach C^∞ within the small gap in (10) only if the bandwidth occupancy is contained in an interval that grows linearly with $\sqrt{\frac{B_c T_c}{\log(B_c T_c)}}$, as suggested by (9), and the error term $o(\frac{1}{\delta B})$ in Lemma 3 can be substituted with an equivalent term $o\left(\sqrt{\frac{\log(B_c T_c)}{B_c T_c}}\right)$.

Lemma 4. *In a wideband non-coherent Rayleigh fading channel, the maximum rate in (10) is achievable at a critical bandwidth occupancy $(\delta B)_{\text{crit}}$ that resides in the range*

$$(\delta B)^- \leq (\delta B)_{\text{crit}} \leq (\delta B)^+, \quad (13)$$

where

$$\begin{aligned} (\delta B)^- &= \frac{P}{N_0} \frac{1}{2\sqrt{(N_t + N_r) \log \pi}} \sqrt{\frac{B_c T_c}{\log(B_c T_c)}} + o\left(\sqrt{\frac{B_c T_c}{\log(B_c T_c)}}\right), \\ (\delta B)^+ &= \frac{P}{N_0} 2\sqrt{\frac{(N_t + N_r)}{N_t^2} \log \pi} \sqrt{\frac{B_c T_c}{\log(B_c T_c)}} + o\left(\sqrt{\frac{B_c T_c}{\log(B_c T_c)}}\right). \end{aligned} \quad (14)$$

Proof: See Appendix G. ■

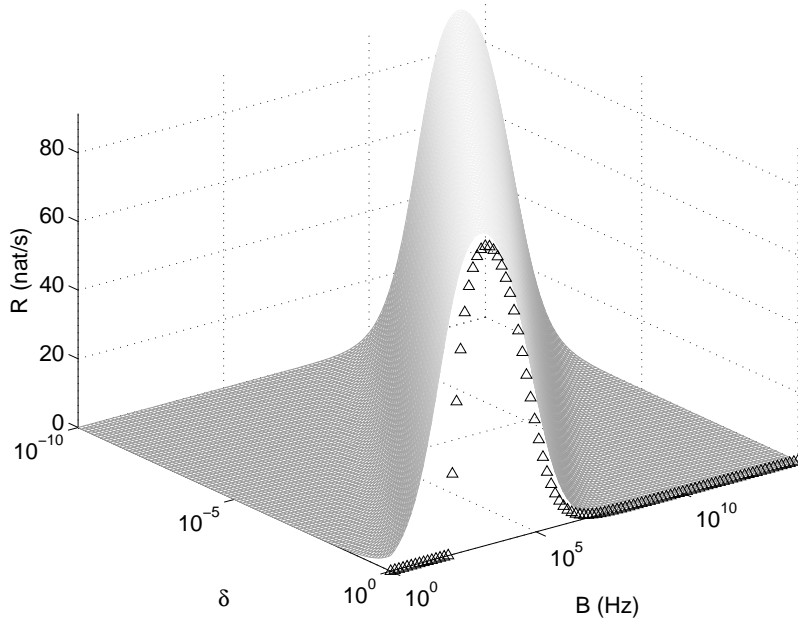
E. Interpretation of the Result

Our upper and lower bounds on $C(B, \delta)$ are all derived from the chain rule

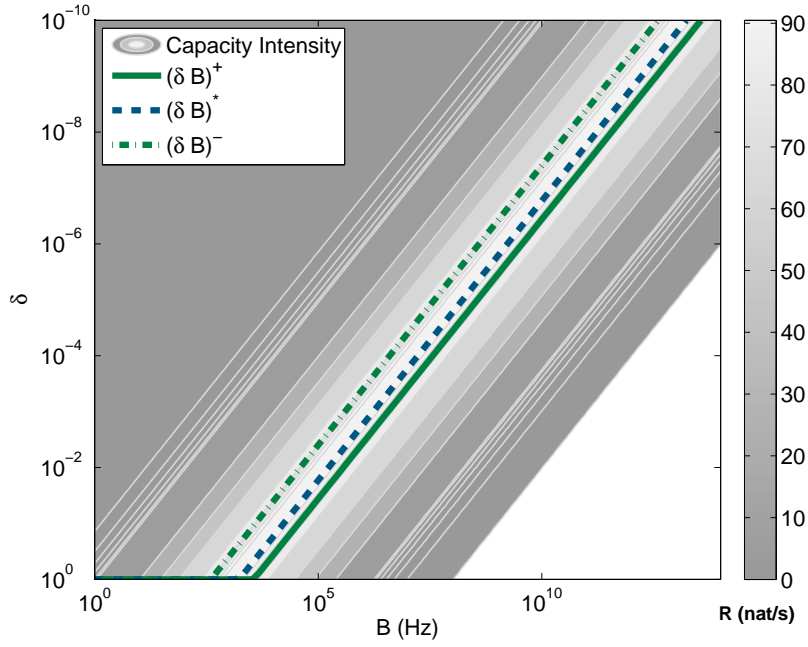
$$I(\mathbf{x}; \mathbf{y}|c) = \delta I(\mathbf{x}, \mathbf{H}; \mathbf{y}|c=1) - \delta I(\mathbf{H}; \mathbf{y}|\mathbf{x}, c=1),$$

where the first term corresponds to the data transmission setup that quantifies the information about $\mathbf{H}\mathbf{x}$ contained in \mathbf{y} and the second term can be interpreted as a “channel estimation” setup that quantifies the rate penalty for not knowing \mathbf{H} . Both terms grow as δB increases but the first term grows faster when δB is small, thus increases $I(\mathbf{x}; \mathbf{y}|c)$, until the second term “accelerates”. Beyond the critical point $(\delta B)_{\text{crit}}$, the second term grows faster than the first, thus erodes $I(\mathbf{x}; \mathbf{y}|c)$, until the capacity drops to zero when $\delta B \rightarrow \infty$. This behavior is illustrated in Fig. 2 for both the capacity upper and lower bounds. The coherence time T_c and coherence bandwidth B_c of the channel jointly determine the relative speeds of this “race” through their product. The factor $T_c B_c$ appears in rate penalty both as the denominator outside the logarithm (there are $T_c B_c$ times fewer i.i.d. channel realizations than signal realizations) and as a multiplier of the SNR inside the logarithm (the power of $T_c B_c$ signal realizations can be combined to estimate each channel realization), leading to a capacity gap depending on $\frac{\log B_c T_c}{B_c T_c}$.

In Fig. 3(a) we represent the upper bound to capacity as a field over the 2D plane (δ, B) with $B_c T_c = 10^3$ and $P/N_0 = 20$ dB. In the vertical cut for $\delta = 1$ we also plot the lower bound using triangular bullets. Note that we intentionally choose a smaller value of P/N_0 to illustrate the details of the transition phase in capacity, which would otherwise be difficult to observe



(a) Upper bound for (δ, B) and the lower bound for $\delta=1$.



(b) Contour plot and levels of bandwidth occupancy.

Figure 3. Capacity upper bound over the plane (δ, B) and the low bound for $\delta=1$, with $B_c T_c = 10^3$, $N_t=N_r=1$, and an intentionally chosen small value $P/N_0=20\text{dB}$. Range of critical bandwidth occupancy is also shown.

with typical values of $P/N_0 \sim 70$ dB [7]. On the B -axis, we can see that for fixed values of

δ the capacity as a function of bandwidth is bell-shaped, grows at small bandwidth, reaches a maximum and then decreases to zero. Fig. 3(b) provides a better perspective on the value of capacity upper bounds as a function of the bandwidth occupancy δB , where the optimal $(\delta B)^*$ that maximizes the capacity lower bound R^{LB} and the range $[(\delta B)^-, (\delta B)^+]$ for the critical bandwidth occupancy $(\delta B)_{\text{crit}}$ are also plotted. For different level of peakiness δ , the peak values of capacity are the same but appear at different bandwidth B , and in fact all points with identical value δB have the same lower/upper bounds. Our analysis recovers previous results for non-peaky signals by setting $\delta=1$, producing a finite critical bandwidth. It also recovers the capacity with infinite-fourth-moment signals by taking $\delta \rightarrow 0$, which drives the critical bandwidth occupancy point further into higher bandwidths satisfying $\lim_{\delta \rightarrow 0} \frac{(\delta B)_{\text{crit}}}{\delta} = \infty$.

Our analysis also unveils the impact of the dimensions of the MIMO array on the non-coherent wideband fading channels. The maximum rate in Lemma 2, derived under the condition that $N_t < B_c T_c$, depends critically on channel coherence $B_c T_c$. For example, for $B_c T_c = 10^3$ and $B_c T_c = 10^6$, the maximum rate (10) can be approximated as, respectively,

$$R(B_c T_c = 10^3) \simeq \frac{P N_r}{N_0} (1 - 0.1 \sqrt{N_t + N_r}), \quad R(B_c T_c = 10^6) \simeq \frac{P N_r}{N_0} (1 - 0.005 \sqrt{N_t + N_r}).$$

When $N_r > 1$ is fixed, increasing the number of transmit antennas will degrade the rate, with the gap growing linearly with $\sqrt{N_t + N_r}$. When $N_t > 1$ is fixed and channel is relatively flat (hence $B_c T_c$ is large), the rate gap is negligible for typical MIMO setups and therefore the rate grows almost linearly with N_r . When the channel is rather dispersive (hence $B_c T_c$ is small), however, increasing N_r will produce a power gain that increases the rate at speed N_r but at the same time will bring in more channel uncertainty that increase the penalty at rate proportional to $\sqrt{N_t + N_r}$. Therefore using too many receive antennas will hurt the achievable rate. For example, the maximum rate peaks around $N_r = 40$ for $B_c T_c = 10^3$. It must be noted that our analysis is accurate for conventional MIMO systems with $N_t < B_c T_c$, and extension to high-dimensional MIMO is out of the scope of the current paper.

IV. UNIFIED CAPACITY FOR PEAKY AND NON-PEAKY SIGNALS

In this section we will show that the peak rate $R^{LB}((\delta B)^*)$ in (10), which is derived by combining non-peaky signaling analysis [7] and tunable peakiness through duty cycle $\delta \in (0, 1]$, approaches C^∞ within the same gap as in the unconstrained capacity $C(B)$ analysis using a

generalized polynomial rate approximation (2) obtained via peaky signaling analysis [8], [9]. We first replace δ , a free parameter in our model representing the duty cycle, with an assigned value $\delta = \text{SNR}^{1-\alpha}$ as in [9], where $\text{SNR} \triangleq P/(BN_0)$ and α is the exponent that determines the wideband slope. This substitution will show that, when the channel coherence length is large, i.e., $B_c T_c \gg 1$, the gaps to C^∞ in (10) and in (2) have the same value at points $(B, \delta = \text{SNR}^{1-\alpha})$. Furthermore, we show that the sufficient and necessary conditions on the coherence length $B_c T_c$ to approach C^∞ , proved in [9, Th. 1-Th. 3], can also be established using our results. Once we have established that the results are equivalent, the opposite path can be taken and use the values of α obtained in [9] to calculate a new range of the critical bandwidth occupancy in closed-form expressions. We discuss the relationship of the two expressions, which have minor differences in the error terms of the calculation of α , reveal a trade-off between accuracy and resolution in [9], and demonstrate that the two methods represent the same optimal rate.

A. Different Analyses Show the Same Results

The analysis in [9] obtains a necessary and sufficient condition on the coherence length of the channel, $B_c T_c$, to guarantee that capacity is above a polynomial of $\text{SNR} = \frac{P}{N_0 B}$ as $B \rightarrow \infty$ with specified peakyness $\delta = \text{SNR}^{\alpha-1}$. This result is given in [9, Th. 3], which is rewritten in the next lemma for easy reference. The result is valid for arbitrary $B_c T_c$, but the necessary condition to approximate C^∞ is akin to requiring that $B_c T_c$ be large.

Lemma 5 (Th. 3 [9]). *For any $\alpha \in (0, 1]$ and $\epsilon \in (0, \alpha)$ the capacity of a Rayleigh block-fading MIMO channel with coherence time T_c , coherence bandwidth B_c , and average signal to noise ratio $\text{SNR} = \frac{P}{BN_0}$ is*

$$\frac{C(B)}{B} \geq N_r \text{SNR} - \frac{N_r(N_r + N_t)}{2N_t} \text{SNR}^{1+\alpha} + \Theta(\text{SNR}^{1+\alpha+\epsilon}), \quad (15)$$

if and only if there exists a $\sigma \in (0, \epsilon)$ such that

$$B_c T_c = \frac{N_t^2}{(N_r + N_t)^2} \text{SNR}^{-2(\sigma+\alpha)}. \quad (16)$$

Recall that in Sec. III, our rate lower bound in (8) contains three terms, the wideband capacity C^∞ , a non-linear rate penalty due to $\log(1 + \text{SNR})$, and a rate penalty due to lack of CSIR. Below the optimal bandwidth occupancy $(\delta B)^*$, the third term of (8) is smaller in absolute value than the second. Replacing the third term by the second term and substituting $\delta = \text{SNR}^{1-\alpha}$, $\alpha \in (0, 1)$

into (8) produces the following sufficient condition in terms of the bandwidth occupancy δB , as stated in Corollary 1.

Corollary 1. *If $\delta B \leq (\delta B)^*$, the achievable rate is lower bounded by*

$$C(B, \delta) \geq \frac{PN_r}{N_0} \left[1 - \left(\frac{P}{BN_0} \right)^\alpha \frac{(\kappa - 2 + N_t + N_r)}{N_t} \right]. \quad (17)$$

On the other hand, above $(\delta B)_{\text{crit}}$, the third term of (8) is greater than the second. This means that $C(B, \delta)$ is smaller than (17), which leads to the necessary condition in Corollary 2.

Corollary 2. *In Rayleigh fading ($\kappa=2$), if $\delta = \text{SNR}^{1-\alpha}$ and if*

$$C(B, \delta) \geq \frac{PN_r}{N_0} \left[1 - \left(\frac{P}{BN_0} \right)^\alpha \frac{(N_t + N_r)}{N_t} \right], \quad (18)$$

then the bandwidth occupancy satisfies $\delta B < (\delta B)^+$.

Now we can use the necessary condition in Corollary 2 and the sufficient condition in Corollary 1 on bandwidth occupancy δB to prove the sufficient and necessary condition (16).

Proposition 1. *Corollary 1 implies the sufficient condition (16) for Lemma 5.*

Proof: Substituting $\delta = \text{SNR}^{1-\alpha}$ and $\kappa=2$ into (9), we can rewrite $\delta B < (\delta B)^*$ in Corollary 1 as

$$B_c T_c > \frac{N_t^2}{(N_r + N_t)^2} \text{SNR}^{-2\alpha} (N_r + N_t) \log(B_c T_c).$$

Since $(N_r + N_t) \log(B_c T_c)$ is a constant and $B \rightarrow \infty$, we have $(N_r + N_t) \log(B_c T_c) \leq \text{SNR}^{-2\epsilon}$ for any $\epsilon > 0$. Therefore, it is also sufficient to have

$$B_c T_c \geq \frac{N_t^2}{(N_r + N_t)^2} \text{SNR}^{-2(\alpha+\epsilon)},$$

which is a sufficient condition that Lemma 5 transforms in the upper limit of $\sigma \leq \epsilon$. ■

Proposition 2. *Corollary 2 implies the necessary condition (16) for Lemma 5.*

Proof: The necessary condition $\delta B < (\delta B)^+$ in Corollary 2 can be rewritten as

$$B_c T_c > \frac{N_t^2}{(N_r + N_t)^2} \text{SNR}^{-2\alpha} \frac{(N_r + N_t)}{4 \log \pi} \log(B_c T_c).$$

Therefore we can express the necessary condition that Lemma 5 sets as lower limit of $\sigma \geq 0$,

$$B_c T_c > \frac{N_t^2}{(N_r + N_t)^2} \text{SNR}^{-2\alpha},$$

as long as $\frac{(N_r + N_t)}{4 \log \pi} \log(B_c T_c) \geq 1$, i.e., $B_c T_c \geq \pi^{4/(N_r + N_t)}$, which is always satisfied in wideband fading channels where $B_c T_c$ is very large, and thus $B_c T_c > \pi^2$. ■

Remark 4. From Proposition 1 and Proposition 2, it is not surprising that the power gain term $\log(B_c T_c)$ was lost in [9], because this sub-polynomial variation of the result has been “buried” in the range of valid exponents ϵ of the error term $O(\text{SNR}^{1+\alpha+\epsilon})$.

B. New Bounds on $(\delta B)_{\text{crit}}$ using the Subquadratic Polynomial Rate Approximation

In our analysis, Lemma 2 prescribes a near-linear-in-power capacity lower bound which can be achieved by all signaling schemes with (δ, B) as long as the bandwidth occupancy δB equals some constant $(\delta B)_{\text{crit}}$. Our analysis does not provide the exact value of $(\delta B)_{\text{crit}}$, but rather bounds it within $[(\delta B)^-, (\delta B)^+]$ in Lemma 4. On the other hand, the result in [9, Th. 3], reproduced here as Lemma 5, prescribes an entire family of parametrized bounds where the parameter ϵ controls both the error term of the generalized Taylor expansion and the resolution of bounding brackets around $(\delta B)_{\text{crit}}$. Corollary 3 makes this explicit.

Corollary 3. The necessary and sufficient condition (16) of Lemma 5 shows that coherent capacity C^∞ is approached by transmitting signals with bandwidth occupancy δB within the limits

$$\delta B < \frac{P}{N_0} \frac{N_r + N_t}{N_t} \sqrt{B_c T_c} \triangleq (\delta B)^{\text{max}}, \quad (19)$$

$$\delta B > \frac{P}{N_0} \left(\frac{N_r + N_t}{N_t} \sqrt{B_c T_c} \right)^{\frac{\alpha}{\alpha+\epsilon}} \triangleq (\delta B)_\epsilon^{\text{min}}. \quad (20)$$

Proof: Substituting $B_c T_c$, $\delta = \text{SNR}^{1-\alpha}$ and $\text{SNR} = \frac{P}{BN_0}$ into (16), we can obtain (19) and (20) by the fact that $\sigma > 0$ and $\sigma < \epsilon$, respectively. ■

Therefore for a given α , which controls the level of peakiness δ and determines the wideband slope, we can observe a clear tradeoff, parametrized by $\epsilon \in (0, \alpha)$, between the accuracy of the Taylor polynomial and the resolution of the bandwidth brackets:

- 1) The **accuracy** of the capacity lower bound calculated in Lemma 5 is determined by the ratio between $\text{SNR}^{1+\alpha}$ and the error term $O(\text{SNR}^{1+\alpha+\epsilon})$. The larger ϵ , the better the approximation, since the error term will vanish faster as $B \rightarrow \infty$.
- 2) The **resolution** of the interval where $(\delta B)_{\text{crit}}$ is contained, $[(\delta B)_{\epsilon}^{\min}, (\delta B)_{\epsilon}^{\max}]$, is determined by the width of the interval. The smaller ϵ , the better the resolution, as the lower boundary $(\delta B)_{\epsilon}^{\min}$ will increase and become tighter when ϵ becomes smaller.

C. Comparison of Critical Bandwidth Occupancy Estimators

So far we have characterized the critical bandwidth occupancy $(\delta B)_{\text{crit}}$ in two different ranges: by a pair of bracket $[(\delta B)^-, (\delta B)^+]$, in our analysis in Lemma 4; and by a parametric interval $[(\delta B)_{\epsilon}^{\min}, (\delta B)_{\epsilon}^{\max}]$, derived from [9, Th. 3] in Corollary 3. To explore the relationship between the two estimators, we compare the difference in the estimated value of α that each analysis produces. We do this because the exponent α provides a unique relation between B and $\delta = \text{SNR}^{1-\alpha} = (\frac{P}{N_0 B})^{1-\alpha}$, allowing for scalar comparison of the methods.

We begin by representing α according to [9, Th. 3]. From (16) in Lemma 5, for given values of the coherence block length $B_c T_c$ and bandwidth $B \in [(\delta B)_{\epsilon}^{\min}, (\delta B)_{\epsilon}^{\max}]$ can be written as

$$\sigma + \alpha = \frac{\log(\frac{(N_t + N_r)^2}{N_t^2} B_c T_c)}{2 \log(\text{SNR}^{-1})}. \quad (21)$$

From the fact that $\sigma > 0$ we get

$$\alpha < \alpha_{\max} \triangleq \frac{\log(\frac{(N_t + N_r)^2}{N_t^2} B_c T_c)}{2 \log(\text{SNR}^{-1})}, \quad (22)$$

and from the fact that $\sigma < \epsilon < \alpha$ we get

$$\alpha > \max\left(\frac{\alpha_{\max}}{2}, \alpha_{\min}(\epsilon)\right), \text{ where } \alpha_{\min}(\epsilon) \triangleq \frac{\log(\frac{(N_t + N_r)^2}{N_t^2} B_c T_c)}{2 \log(\text{SNR}^{-1})} - \epsilon. \quad (23)$$

Note that when ϵ decreases, $\alpha_{\min}(\epsilon)$ increases such that the range of α becomes smaller but at the same time the error term $O(\text{SNR}^{1+\alpha+\epsilon})$ vanishes more slowly: improving the *resolution* of the bandwidth occupancy range comes at the price of decreasing the *accuracy* of the capacity polynomial approximation. We can make an approximate selection of ϵ such that polynomial error term is in the order of a p -percent of the term $\text{SNR}^{1+\alpha}$, i.e., finding $\epsilon(p)$ such that

$$\text{SNR}^{1+\alpha} > \frac{100}{p} \text{SNR}^{1+\alpha+\epsilon(p)}.$$

This generates a family of narrower estimated margins $[\alpha_{\min}(p), \alpha_{\max}]$ parametrized by the pre-selected error percentage $p\%$ by raising the lower bracket.

On the other hand, we can bound α using the critical bandwidth occupancy interval in Lemma 4 in combination with $\delta = \text{SNR}^{1-\alpha}$. With $\delta B = (\delta B)^+$ we get

$$\alpha^+ = \frac{\log\left(\frac{4(N_t+N_r)\log\pi}{N_t^2} \frac{B_c T_c}{\log(B_c T_c)}\right)}{2\log(\text{SNR}^{-1})} = \frac{\log\left(\frac{(N_t+N_r)^2}{N_t^2} B_c T_c\right)}{2\log(\text{SNR}^{-1})} - \frac{\log\left(\frac{(N_t+N_r)\log(B_c T_c)}{4\log\pi}\right)}{2\log(\text{SNR}^{-1})}, \quad (24)$$

and with $\delta B = (\delta B)^-$ we get

$$\alpha^- = \frac{\log\left(\frac{1}{4(N_t+N_r)\log\pi} \frac{B_c T_c}{\log(B_c T_c)}\right)}{2\log(\text{SNR}^{-1})} = \frac{\log\left(\frac{(N_t+N_r)^2}{N_t^2} B_c T_c\right)}{2\log(\text{SNR}^{-1})} - \frac{\log(4\log\pi \frac{(N_t+N_r)^3}{N_t^2} \log(B_c T_c))}{2\log(\text{SNR}^{-1})}. \quad (25)$$

Recall that for any $\epsilon > 0$ we have $(N_t + N_r)\log(B_c T_c) \leq \lim_{\text{SNR} \rightarrow 0} \text{SNR}^{-2\epsilon}$. This means that we can show that $\alpha_{\max} > \alpha^+ > \alpha_{\min}(\epsilon)$, and the interval between the three vanishes as $\epsilon \rightarrow 0$.

Remark 5. *All the results coincide in that $\alpha \propto \log(B_c T_c)$, making capacity of channels with low $B_c T_c$ approach their wideband limit very slowly with $\text{SNR} \rightarrow 0$ and channels with high $B_c T_c$ approach the wideband limit faster. This is the main intuition of the results in [9]: non-coherent channels approach the coherent channel capacity when coherence length is large enough.*

D. Illustration

We plot the capacity lower bound on the plane (δ, B) in Fig. 4 for $B_c T_c = 10^6$ (first graph) and for $B_c T_c = 10^4$ (second graph). The peak capacity is achievable in a region with constant product δB , starting at relatively large bandwidths, and both estimations of the optimal region are narrow. The choice of ϵ determines the polynomial lower bound and therefore the range $[\alpha_{\min}(\epsilon), \alpha_{\max}]$. We can generate a set of estimations $\alpha_{\min}(\epsilon)$ by fine-tuning ϵ within the range $(0, \alpha)$, as shown by the curves corresponding to $\alpha_{\min}(\epsilon)$ with $\epsilon = \alpha/2, \alpha/4$, respectively. Note that the conservative choice $\epsilon = \alpha$ leads to the widest possible range for $[\alpha_{\max}/2, \alpha_{\max}]$. On the other hand, the resolution of the estimators from our own analysis $[\alpha^-, \alpha^+]$ depends only on the value of $B_c T_c$, and its range becomes smaller as $B_c T_c$ increases.

Since the resolution of the estimation by $[\alpha^-, \alpha^+]$ relies on $B_c T_c$ and the relative margin of $[\alpha_{\min}, \alpha_{\max}]$ depends on ϵ , we show in Fig. 5 the evolution of the two boundary methods with ϵ and $B_c T_c$. The method [9] produces the highest upper bound α_{\max} that does not change, and a family of lower bounds $\alpha_{\min}(p)$ depicted in the figure for errors of 1% and 10% and its lowest

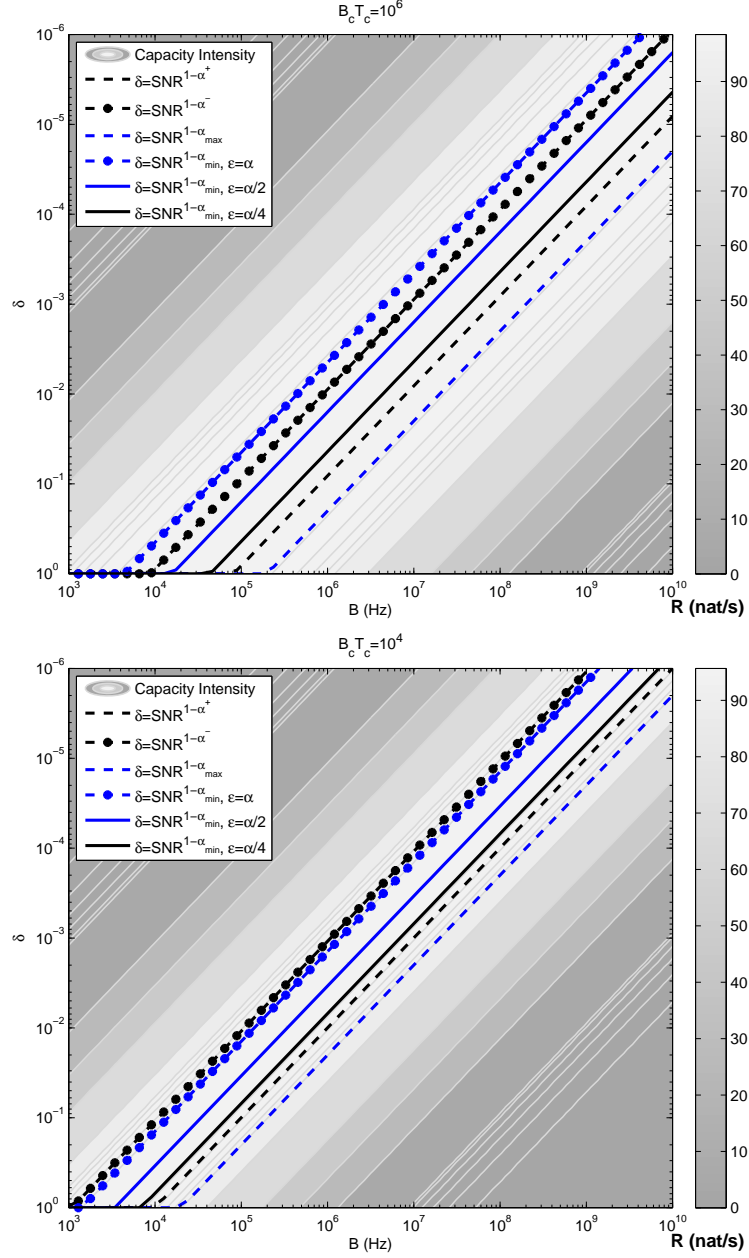


Figure 4. Capacity lower bound on the plane (δ, B) with $P/N_0=20\text{dB}$, $B_c T_c=10^6$ (first graph) and $B_c T_c=10^4$ (second graph). Curves with $\alpha_{\min}(\epsilon)$ are generated with $\epsilon=\alpha, \alpha/2, \alpha/4$, respectively.

bound $\alpha_{\max}/2$. Note that at low coherence length, $B_c T_c$, the limit $\alpha_{\min} > \alpha_{\max}/2$ makes it impossible to select values of ϵ corresponding with a polynomial accuracy of 1%, and then 10%. This shows that the polynomial rate with peaky signaling in [9] also displays a gap from C^∞ decreasing with $B_c T_c$. On the other hand, the critical bandwidth occupancy method produces

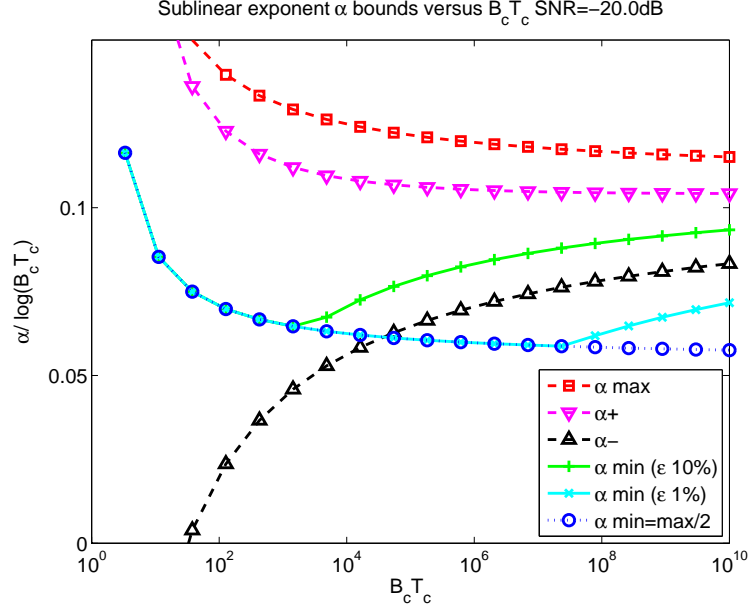


Figure 5. Evolution of $\frac{\alpha}{\log(B_c T_c)}$ versus $B_c T_c$ with SNR = -20dB.

boundaries that are loose at low coherence length but improve significantly when this parameter grows and that do not pay for tightness a price in accuracy of the polynomial approximation.

V. CONCLUSIONS

In this paper we have unified the study of the rate approximations to C^∞ for peaky and non-peaky signaling in non-coherent wideband fading channels where energy rather than spectrum is the limiting resource. We have generalized the critical bandwidth analysis [7] to families of signaling schemes with varying bandwidth B and transmission duty-cycle $\delta \in (0, 1]$ to allow arbitrary levels of signal peakiness. We introduce the metric of bandwidth occupancy to measure the average bandwidth usage over time and define it as δB , the product between the bandwidth and the fraction of time it is in use. Our main result shows the existence of a fundamental limit on the bandwidth occupancy in non-coherent channels for any level of signal peakiness. For all signaling schemes with the same bandwidth occupancy, as the bandwidth occupancy approaches its critical value $(\delta B)_{\text{crit}}$, rates converge with the same asymptotic behavior to the

same almost-linear in power value (measured in nats/s)

$$C(B, \delta = \frac{(\delta B)_{\text{crit}}}{B}) \geq \frac{PN_r}{N_0} \left[1 - \sqrt{\frac{1 + \log(B_c T_c)}{B_c T_c} (\kappa - 2 + N_t + N_r) \log \pi} \right],$$

where T_c is the coherence time and B_c is the coherence bandwidth. The rates decrease to zero as the bandwidth occupancy goes to infinity. Moreover, we provide upper and lower bounds to this critical value. The bounds have the same growth with $B_c T_c$ and $\frac{P}{N_0}$, and they only differ on a constant term.

To characterize the relation between the capacity with a tunable peakiness constraint $C(B, \delta)$ and the unconstrained non-coherent wideband capacity $C(B)$, we rewrite the above capacity expression as a polynomial equivalent to the analysis in [9]. We have recovered the results in [9, Th. 1-Th. 3] and obtained the almost-linear polynomial expressions for capacity in the limit $\delta B \rightarrow (\delta B)_{\text{crit}}$ with a dominant sub-linear term SNR^α . As the bandwidth occupancy approaches the limit, capacity approaches the power-limited wideband limit with a speed of convergence determined by $\text{SNR}^{1+\alpha}$, which approaches that of coherent channels as $B_c T_c \rightarrow \infty$. The fundamental nature of the bandwidth occupancy measure reflects the fact that capacity of any signaling scheme is contained within the same bounds as long as the product δB is constant.

Within this framework, limited bandwidth transmission with non-peaky signaling and unlimited bandwidth transmission with peaky signaling, which have been treated as very different schemes, are shown to be merely two extreme points in a continuous range of transmission strategies within the same bounds as long as they have the same amount of bandwidth occupancy. This suggest that for the practical goal of operating at a *rate very close to* C^∞ , all pairs (B, δ) with the optimal occupancy do not exhibit significant differences. Achieving capacity, i.e. the supremum rate, may on the other hand only be possible in some specific distributions. The selected peakiness $\delta = \text{SNR}^{1-\alpha}$ in [9] becomes invalid if $\text{SNR} > 1$ (as $\delta \leq 1$ by design), whereas our model determines peakiness through $\delta B < (\delta B)_{\text{crit}}$, a quantity that is well defined for all values of SNR. This gives the intuition that below the critical point it would be questionable to claim that the frequency-selective channel is in the wideband regime, and therefore regular non-peaky transmissions with full bandwidth occupancy must be employed. Beyond the critical point, both signaling schemes provide the same capacity limit.

We have shown that most of the advantage of peaky signaling stems from harnessing power for long periods of time to transmit some infrequent flashes with boosted power, without encoding

information in the position of the active symbols as in ON/OFF modulations. Moreover, this power boost does not in fact outperform non-peaky transmission with the optimal bandwidth, which means that in practical systems the amount of peakiness and the bandwidth may be chosen at will as long as the maximum occupancy level is respected.

Our analysis has some limitations. Firstly, the potential spatial correlation among MIMO antennas is not accounted for. Secondly, although our capacity lower bounds are valid for general fading channels, our upper bound and critical bandwidth occupancy expressions assume Rayleigh fading. Besides, the performance of a signaling system with practical channel estimation techniques [22], peak constrained signals [11], [15], [19], [23], finite modulation options, and non-ideal decoders may be degraded as compared to the theoretical bounds provided in this paper.

APPENDIX A

JUSTIFICATION OF OUR FADING MODEL CHOICE

As a general case, a wireless channel is modeled as a set \mathcal{L} of paths, where each path $\ell \in \mathcal{L}$ is defined by a group delay τ_ℓ , a phase of arrival θ_ℓ , and an impulse response $h_\ell(t)$. For a pair of antennas (u, v) with received signal $r^{(v)}(t)$ and transmitted signal $s^{(u)}(t)$, we have

$$r^{(v)}(t) = s^{(u)}(t) * \sum_{\ell \in \mathcal{L}} h_\ell^{(u,v)}(t - \tau_\ell^{(u,v)}) e^{j\theta_\ell^{(u,v)}} + z^{(v)}(t) = s^{(u)}(t) * h^{(u,v)}(t) + z^{(v)}(t), \quad (26)$$

where $z^{(v)}(t)$ is the AWGN noise, and the channel delay spread D and coherence time T_c are determined by the aggregate channel impulse response $h^{(u,v)}(t)$. Traditionally, $h_\ell^{(u,v)}(t)$ s are scalar gains or narrow pulses that can be approximated by the Dirac delta function, in which case the set \mathcal{L} would be a sort of “ray tracing” of perfect reflections of the signal with a scalar gain. However, recent mmWave measurements have found much higher delay-spread values [24] than those predicted in ray-tracing calculations [25]. This may be due to rich scattering from small objects in mmWave fading channels, which are not so sparse in practice. This is due to the fact that, although there are few arrival direction “clusters”, in each cluster energy arrivals spread along many angular directions [26]. Therefore each arrival direction sees the additive effect of a large number of scattered reflections, not a single path, and each $h_\ell^{(u,v)}(t)$ has a delay spread, instead of a scalar channel gain. The construction of discrete-time system models falls into the following three regimes depending on the sampling rate:

- Sampling $h^{(u,v)}(t)$ at low rate, all the energy in the delay spread D would be captured by a single sampling interval, so the resulting discrete channel would be a scalar coefficient, which is approximately Gaussian distributed due to the law of large numbers. This is called the **narrowband**, or **frequency-flat** channel.
- Sampling at higher rate would make the energy in D be captured in multiple sampling intervals, each with an independent scalar coefficient. This is called the **wideband** channel, or **frequency selective** with rich scattering environment.
- The third regime occurs when the number of sampling bins is much larger than the number of paths in \mathcal{L} . The sampled channel coefficients are sparse and not Gaussian distributed. This is called the **ultra-wideband**.

We consider the wideband fading model to be relevant in mmWave communications where rich scattering and longer delay spread was observed [24]. Our discrete equivalent channel is derived from the propagation described above by employing the classic framework of a Nyquist sampling at frequency B , the consideration of frequency-domain signaling with a K -point DFT, satisfying $K = BT_c$, and a cyclic prefix of negligible duration $M = B/B_c = K/B_c T_c \ll K$. The same channel model is employed in [7].

APPENDIX B

COMPATIBILITY WITH ANOTHER COMMON MODEL

In [9] the signals are divided into a set of $M = B/B_c$ narrowband channels (a.k.a. frequency bins) with encoding symbols defined with a symbol period of $1/B_c$. Each narrowband channel can be perfectly sampled at a rate of just 1 sample per symbol period, and there are M parallel frequency bands that produce M samples per symbol period. In this scheme multiple symbols see the same channel realization and the channel coherence length is a block of $L_c = T_c B_c$ consecutive symbols. By indexing with m the independent frequency bins and with ℓ the consecutive periods on the same channel block realization, we get the model

$$\mathbf{y}[m, \ell] = \mathbf{H}[m, \ell] \mathbf{x}[m, \ell] + \mathbf{z}[m, \ell], \quad (27)$$

where $\mathbf{H}[m, \ell]$ remains unchanged for $\ell = 1, \dots, L_c$. To exploit channel coherence, the encoding process must design the transmitted signal for the L_c consecutive symbols jointly, and the

encoding model is represented with matrices as

$$\mathbf{Y}[m] = \mathbf{H}[m]\mathbf{X}[m] + \mathbf{Z}[m], \quad (28)$$

where the dimensions are $N_r \times L_c = (N_r \times N_t)(N_t \times L_c)$.

In this model, for every encoding interval of length L_c and across all M frequency bins there are a total of $ML_c=K$ complex valued coefficients. Therefore, this channel model provides exactly the same number of signaling dimensions for transmission as the model we have derived. But the representations of the channel variation are different. In this model there are fewer channel coefficients, each of them is i.i.d. and identically repeated for every L_c consecutive symbols. Whereas our derived model (5) supports any type of channel correlation, not only repetition, as long as there are K correlated coefficients generated by a fraction $1/B_cT_c$ of independent random variables. It is possible to represent the system model (28) with repeated identical channel coefficients in our derived model format by replacing the matrix notation $\mathbf{H}[m]\mathbf{X}[m]$ with our vectorized notation $\mathbf{H}\mathbf{x}$ where \mathbf{H} is a block-diagonal matrix with the values of $\mathbf{H}[m]$ in its main diagonal and zeros in the upper and lower triangles as in (4).

APPENDIX C

EQUIVALENCE IN SIGNALING REPRESENTATION

Our channel model uses Nyquist sampling at the full B and therefore it is able to represent any signal with this bandwidth without loss. For the sake of completeness we will propose the exact formulation to implement a valid signal in the model of [9] (hereafter, filter-bank model) with our model (hereafter, OFDM model) using only preprocessing linear matrices. With this we show that any signal possible in the filter-bank model can be transmitted through the OFDM model, and therefore capacity results in our model are fully compatible.

Without loss of generality, let us assume a SISO channel and unit power to simplify notation. Assume also that the integers $K=\lceil T_cB \rceil$, $M=\lceil B/B_c \rceil$ and $L_c=\lceil T_cB_c \rceil$ are satisfied exactly so we may use simply $K=ML_c$. In continuous time, the filter-bank model is represented in

$$r(t) = \sum_{i=-\infty}^{\infty} \delta(t-iT_c) * \left(\sum_{\ell=0}^{L_c-1} \delta(t-\ell/B_c) * \left(\sum_{m=0}^{M-1} h_i[m, \ell] x_i[m, \ell] \text{sinc}(tB_c) e^{-j2\pi m B_c t} \right) \right) + z(t), \quad (29)$$

where multiplication by $h_i[m, \ell]$ and $x_i[m, \ell]$ assigns the scalar value received in each frequency bin $m \in \{0, \dots, M-1\}$ and in each transmit symbol period $\ell \in \{0, \dots, L_c-1\}$.

We separate the encoding for each channel block realization indexed by i , drop the index, and use the fact that the channel coefficient in each frequency bin remains the same for all symbols to take away the index ℓ from $h[m]$. This gives

$$y(t) = \sum_{\ell=0}^{L_c-1} \delta(t-\ell/B_c) * \left(\sum_{m=0}^{M-1} h[m]x[m, \ell] \text{sinc}(tB_c) e^{j2\pi m B_c t} \right) + z(t). \quad (30)$$

With this continuous-time signal, we apply Nyquist sampling at rate B to generate $K=BT_c$ samples per sequence. Notice that for integer $M=B/B_c$, the discrete sinc function is $\text{sinc}[n/M] \triangleq \text{sinc}(\frac{nB_c}{B})$ and the delta delay on index n is ℓM . We can represent (30) by

$$y[n] = \sum_{\ell=0}^{L_c-1} \delta[n-\ell M] * \left(\sum_{m=0}^{M-1} h[m]x[m, \ell] \text{sinc}\left[\frac{n}{M}\right] e^{j2\pi \frac{n}{K} m L_c} \right) + z[n], \quad n = 0, \dots, K-1. \quad (31)$$

We compute the K -point DFT,

$$y[k] = \sum_{\ell, m} e^{-j2\pi \frac{k\ell}{L_c}} h[m]x[m, \ell] \text{rec}[k/L_c - m] + z[k]. \quad (32)$$

The rectangular window equals one only when $\lfloor k/L_c \rfloor = m$. By representing $k < K$ as $k = u * L_c + v$ with $u \triangleq \lfloor k/L_c \rfloor$ and $v \triangleq k \bmod L_c$, we obtain

$$y[k] = h[u] \sum_{\ell=0}^{L_c-1} e^{j2\pi \frac{v\ell}{L_c}} x[u, \ell] + z[k], \quad \text{with} \quad \begin{cases} u = \lfloor k/L_c \rfloor, \\ v = k \bmod L_c. \end{cases}$$

Now we can see that the sum is actually the v th element in the L_c -IDFT of the sequence $x[u, \ell]$.

Since the IDFT of a sequence $\mathbf{a} = (a_1 \dots a_{L_c})^T$ can be written as a matrix product $\text{IDFT}(\mathbf{a}) = \mathbf{F}\mathbf{a}$,

We can represent the system model the same way as our matrix channel notation as

$$\mathbf{y} = \mathbf{H}\Phi\mathbf{x} + \mathbf{z}, \quad (33)$$

where \mathbf{H} for SISO is a $K \times K$ diagonal matrix with its k -th diagonal element $h[u]$, \mathbf{x} is $K \times 1$ with $\mathbf{x}^{(k)} = x[u, v]$. The L_c -IDFT is computed by the block-diagonal square matrix

$$\Phi = \left(\begin{array}{c|cc} \mathbf{F} & \dots & \mathbf{0} \\ \hline \vdots & \ddots & \vdots \\ \hline \mathbf{0} & \dots & \mathbf{F} \end{array} \right). \quad (34)$$

This shows that any channel of the filter-bank model can be represented by the OFDM model using a channel matrix $\tilde{\mathbf{H}} = \mathbf{H}\Phi$. The reciprocal compatibility can be proven by taking a precoding DFT matrix at the transmitter, $\tilde{\mathbf{x}} = \Phi^\dagger \mathbf{x}$, which leads to

$$\mathbf{y} = \tilde{\mathbf{H}}\tilde{\mathbf{x}} = \mathbf{H}\Phi\tilde{\mathbf{x}} = \mathbf{H}\Phi\Phi^\dagger \mathbf{x} = \mathbf{H}\mathbf{x}.$$

The multiplication by Φ^\dagger is unitary, so if the OFDM model uses $\mathbf{x} \sim \mathcal{CN}(\boldsymbol{\mu}, \boldsymbol{\Sigma})$ and Φ is a full- K -rank square orthonormal matrix, then $\Phi^\dagger \mathbf{x} \sim \mathcal{CN}(\Phi^\dagger \boldsymbol{\mu}, \Phi^\dagger \boldsymbol{\Sigma} \Phi)$. Gaussian distribution is maintained when the channel model is changed, and the mutual information results for both channel models supported by our bounds based on Gaussian inputs are completely equivalent.

APPENDIX D

PROOF OF LEMMA 1

Since the receiver knows which phase the duty cycle is in (e.g., scheduled according to a pseudo-random sequence), the rate can be determined via the chain rule

$$\frac{1}{T_c} \mathbf{I}(\mathbf{x}; \mathbf{y}|c) = \frac{\delta}{T_c} \mathbf{I}(\mathbf{x}; \mathbf{y}|c=1) + (1-\delta) \cdot 0 = \frac{\delta}{T_c} \mathbf{I}(\mathbf{x}, \mathbf{H}; \mathbf{y}|c=1) - \frac{\delta}{T_c} \mathbf{I}(\mathbf{H}; \mathbf{y}|\mathbf{x}, c=1), \quad (35)$$

where the first step comes from the fact that $\mathbf{H}\mathbf{x}=0$ in the idle block ($c=0$) and $P_r(c=1) = \delta$. During the active block the input follows a Gaussian distribution $\mathcal{CN}(0, \frac{P}{\delta B N_0})$ and the first term in (35) can be lower bounded by

$$\frac{\delta}{T_c} \mathbf{I}(\mathbf{x}, \mathbf{H}; \mathbf{y}|c=1) \geq \frac{\delta}{T_c} \mathbf{I}(\mathbf{x}; \mathbf{y}|\mathbf{H}, c=1) = \delta \times \mathbf{E}_{\mathbf{H}} \left[\frac{1}{T_c} \log \det(\mathbf{I}_{K N_r} + \frac{P}{\delta B N_t N_0} \mathbf{H} \mathbf{H}^\dagger) \right], \quad (36)$$

where the first step is from the non-negativity of mutual information, and the second is due to independence of channel coefficient \mathbf{H} in each subcarrier and transmit antenna. Furthermore,

$$\begin{aligned} \delta \mathbf{E}_{\mathbf{H}} \left[\frac{1}{T_c} \log \det(\mathbf{I}_{K N_r} + \frac{P}{\delta B N_t N_0} \mathbf{H} \mathbf{H}^\dagger) \right] &= \delta \frac{K}{T_c} \mathbf{E}_{\mathbf{H}} \left[\log \det(\mathbf{I}_{N_r} + \frac{P}{\delta B N_t N_0} \hat{\mathbf{H}} \hat{\mathbf{H}}^\dagger) \right] \\ &\stackrel{(a)}{=} \delta \frac{K}{T_c} \sum_{i=1}^{\min(N_t, N_r)} \mathbf{E}_{\mathbf{H}} \left[\log(1 + \frac{P}{\delta B N_t N_0} \lambda_i) \right] \\ &\stackrel{(b)}{\geq} \delta B \mathbf{E}_{\mathbf{H}} \left[\frac{P \operatorname{tr}(\hat{\mathbf{H}} \hat{\mathbf{H}}^\dagger)}{\delta B N_t N_0} - \left(\frac{P}{\delta B N_t N_0} \right)^2 \frac{\operatorname{tr}((\hat{\mathbf{H}} \hat{\mathbf{H}}^\dagger)^2)}{2} \right] \\ &\stackrel{(c)}{=} \frac{P N_r}{N_0} \left[1 - \frac{P/(\delta B)}{2 N_r N_t^2 N_0} \mathbf{E}_H \left[\sum_{t,r} |h_{t,r}|^4 + \sum_{t \neq u, r} |h_{t,r}|^2 |h_{u,r}|^2 + \sum_{t,r \neq v} |h_{t,r}|^2 |h_{t,v}|^2 + \sum_{t \neq u, r \neq v} h_{t,r} h_{u,r}^* h_{t,v}^* h_{u,v} \right] \right] \\ &\stackrel{(d)}{=} \frac{P N_r}{N_0} \left[1 - \frac{P (N_t N_r \kappa + N_t N_r (N_r - 1) + N_r N_t (N_t - 1))}{2 \delta B N_r N_t^2 N_0} \right] \\ &= \frac{P N_r}{N_0} \left[1 - \frac{P}{2 \delta B N_t N_0} (\kappa - 2 + N_t + N_r) \right], \end{aligned} \quad (37)$$

where λ_i are eigenvalues of $\hat{\mathbf{H}} \hat{\mathbf{H}}^\dagger$ with $\hat{\mathbf{H}} = [h_{t,r}]_{N_r \times N_t}$ representing the diagonal blocks of \mathbf{H} , and $h_{t,r}$ is the (r, t) -th element in $\hat{\mathbf{H}}$. Equation (a) comes from the fact that $\mathbf{H}[k]$ are identically

distributed for all $k=0, \dots, K-1$, (b) is due to $\log(1+x) \geq x-x^2/2$ for $x \rightarrow 0$ and the fact that $\sum_i \lambda_i = \text{tr}(\hat{\mathbf{H}}\hat{\mathbf{H}}^\dagger)$ and $\sum_i \lambda_i^2 = \text{tr}((\hat{\mathbf{H}}\hat{\mathbf{H}}^\dagger)^2)$. Equation (c) is by careful rearrangement. Equation (d) comes from $E_{\mathbf{H}}[|h|^2]=1$, $E_{\mathbf{H}}[|h|^4]=\kappa$, $E_{\mathbf{H}}[h]=0$, and independence of matrix entries.

To upper bound the second term we choose \mathbf{H} to be Rayleigh fading (with the maximum entropy) and interpret \mathbf{x} as a pilot signal that gives side information between \mathbf{H} and \mathbf{y} .

$$I(\mathbf{H}; \mathbf{y} | \mathbf{x}, c=1) \leq I(\mathbf{H}_{\text{Gaussian}}; \mathbf{y} | \mathbf{x}_{\text{Pilots Signal}}, c=1) \triangleq \overline{I(\mathbf{H}; \mathbf{y} | \mathbf{x}, c=1)}. \quad (38)$$

An example for channel estimation would be a system where the pilot signal transmitted on antenna u is a uM times delayed version of the signal on antenna 1. After transmitting K pilot symbols, at each receive antenna a K -equation MN_t -unknowns linear estimation problem is established and can be solved using the MMSE estimator.

Let $\Lambda^{(v)}$ be the $MN_t \times MN_t$ diagonal matrix containing in its $uM+m$ diagonal element $g_{uM+m} = E[|h[m]^{(u,v)}|^2]$ (the gain of the m -th channel tap in the (u, v) transmit and receive antenna pair), and let Ξ be a $K \times MN_t$ circulant matrix ($MN_t < K$) containing $\tilde{\mathbf{x}}_{(i-j) \bmod K}$ in its (i, j) -th coefficient, where $\tilde{\mathbf{x}} = \mathbf{x}/\sqrt{P}$ is unit-power pilot signal. Notice that the mention of pilot signals here is to upper bound a mutual information term, rather than implementing a practical channel estimation as required in a coherent receiver. Exploiting the fact that channel estimation is carried out on each receive antenna concurrently based on the hypothetical pilot

signal Ξ from all transmit antennas, we get that the upper bound results in

$$\begin{aligned}
\frac{\delta}{T_c} \overline{\mathbf{I}(\mathbf{H}; \mathbf{y} | \mathbf{x}, c=1)} &= \frac{\delta}{T_c} \sum_{v=1}^{N_r} \mathbf{E} \left[\log \det \left(\mathbf{I} + \frac{P/(\delta B)}{N_t N_0} \Xi^\dagger \Xi \Lambda^{(v)} \right) \right] \\
&\stackrel{(a)}{\leq} \frac{\delta N_r}{T_c} M N_t \mathbf{E} \left[\log \left(\frac{1}{M N_t} \text{tr} \left(\mathbf{I} + \frac{P/(\delta B)}{N_t N_0} \Xi^\dagger \Xi \Lambda^{(1)} \right) \right) \right] \\
&\stackrel{(b)}{=} \frac{\delta B N_r N_t}{B_c T_c} \mathbf{E} \left[\log \left(1 + \frac{P/(\delta B)}{M N_t^2 N_0} \sum_{n=1}^{M N_t} g_n \sum_{k=0}^{K-1} |\tilde{x}[k-n-1]|^2 \right) \right] \\
&\stackrel{(c)}{\leq} \frac{\delta B N_r N_t}{B_c T_c} \log \left(1 + \frac{P/(\delta B)}{M N_t^2 N_0} K \sum_{n=1}^{M N_t} g_n \mathbf{E} \left[\frac{1}{K} \sum_{k=0}^{K-1} |\tilde{x}[k]|^2 \right] \right) \\
&\stackrel{(d)}{=} \frac{\delta B N_r N_t}{B_c T_c} \log \left(1 + \frac{P/(\delta B)}{M N_t^2 N_0} K \sum_{n=1}^{M N_t} g_n \right) \\
&\stackrel{(e)}{\leq} \frac{\delta B N_r N_t}{B_c T_c} \log \left(1 + \frac{P/(\delta B)}{M N_t N_0} K \right) \\
&\stackrel{(f)}{=} \frac{\delta B N_r N_t}{B_c T_c} \log \left(1 + \frac{P}{\delta B N_0 N_t} (B_c T_c) \right), \tag{39}
\end{aligned}$$

where (a) stems from the AM–GM inequality and that channel gains between all antenna pairs are i.i.d, (b) is due to the fact that Ξ is a circulant matrix, which has the same coefficients shifted across all its columns, so its eigenvalues are the DFT coefficients of the columns, (c) is Jensen's inequality, (d) derives from the fact that \tilde{x} has unit power, and (e) is due to the upper bound of squared channel coefficients $\sum_{n=1}^{M N_t} g_n \leq N_t$, and (f) uses $\frac{K}{M} = B_c T_c$.

APPENDIX E

PROOF OF LEMMA 2

Taking partial derivative of (8) w.r.t. the product δB , we obtain

$$\frac{\partial R^{LB}(\delta B)}{\partial(\delta B)} = \frac{P N_r}{N_0} \left[\frac{P(\kappa - 2 + N_t + N_r)}{2(\delta B)^2 N_t N_0} - \frac{N_0 N_t}{P B_c T_c} \log \left(1 + \frac{P B_c T_c}{(\delta B) N_t N_0} \right) + \frac{1}{\delta B \left(1 + \frac{P B_c T_c}{N_0 N_t (\delta B)} \right)} \right]. \tag{40}$$

Near the maximum of $R^{LB}(\delta B)$ the term $\frac{P}{(\delta B) N_0} B_c T_c$ is either $\gg 1$ or $\simeq 1$; because $R^{LB}(\delta B)$ is already approaching zero if $\frac{P}{(\delta B) N_0} B_c T_c \ll 1$. This means we can make the approximation

$$\frac{(\kappa - 2 + N_t + N_r)}{2} \simeq \frac{\log(1 + \frac{P}{(\delta B)^* N_0} B_c T_c)}{(P/(N_t N_0 (\delta B)^*))^2 B_c T_c}, \tag{41}$$

which solves as (9). Evaluating $R^{LB}(\delta B^*)$ and using the same inequality in [7] produces (10).

APPENDIX F
PROOF OF LEMMA 3

We upper bound the first term in (35) enforcing signal bandwidth B and duty cycle δ .

$$\begin{aligned}
\frac{\delta}{T_c} \mathbf{I}(\mathbf{x}, \mathbf{H}; \mathbf{y}|c=1) &\stackrel{(a)}{=} \frac{\delta}{T_c} \mathbf{h}(\mathbf{y}|c=1) - \frac{\delta}{T_c} \mathbf{h}(\mathbf{y}|\mathbf{H}, \mathbf{x}, c=1) \\
&\stackrel{(b)}{=} \frac{\delta}{T_c} \mathbf{h}(\mathbf{H}\mathbf{x} + \mathbf{z}|c=1) - \frac{\delta}{T_c} \mathbf{h}(\mathbf{z}) \\
&\stackrel{(c)}{\leq} \frac{\delta}{T_c} \mathbf{h}\left(\mathcal{CN}(0, \mathbf{I}_{\frac{P}{\delta}} + BN_0)\right) - \frac{\delta}{T_c} \mathbf{h}(\mathbf{z}) \\
&= \delta N_r B \log\left(1 + \frac{P}{\delta B N_0}\right),
\end{aligned} \tag{42}$$

where (a) is from the definition of mutual information; (b) is from the channel model; (c) comes from the fact that \mathbf{z} is independent of \mathbf{x} and \mathbf{H} , and $\mathbf{h}(\mathbf{H}\mathbf{x} + \mathbf{z}|c=1)$ is maximized by a Gaussian distribution under the power constraint $\frac{P}{\delta} + BN_0$. Use the approximation $\log(1+x) = x - x^2/2 + o(x^2)$, we can rewrite (42) as

$$\frac{\delta}{T_c} \mathbf{I}(\mathbf{x}, \mathbf{H}; \mathbf{y}|c=1) \leq \frac{PN_r}{N_0} \left[1 - \frac{P}{2\delta B N_0}\right] + o\left(\frac{1}{\delta B}\right). \tag{43}$$

For the second term of (35), with the Rayleigh fading assumption, the inequality in (38) is met with equality. From there on, upper bounds are found by taking a couple of minimums in the argument of the logarithm.

$$\begin{aligned}
\frac{\delta}{T_c} \mathbf{I}(\mathbf{H}; \mathbf{y}|\mathbf{x}, c=1) &= \frac{\delta}{T_c} \sum_{v=1}^{N_r} \mathbf{E} \left[\log \det \left(\mathbf{I} + \frac{P/(\delta B)}{N_t N_0} \Xi^\dagger \Xi \Lambda^{(v)} \right) \right] \\
&\stackrel{(a)}{\geq} \frac{\delta N_r}{T_c} \mathbf{E} \left[\log \det \left(\mathbf{I} + \frac{P g_{\min}}{\delta B N_t N_0} \Xi^\dagger \Xi \right) \right] \\
&\stackrel{(b)}{=} \sum_{n=1}^{MN_t} \frac{\delta N_r}{T_c} \mathbf{E} \left[\log \left(1 + \frac{P g_{\min}}{\delta B N_t N_0} \lambda_n(\Xi^\dagger \Xi) \right) \right] \\
&\stackrel{(c)}{\geq} \frac{\delta B N_r N_t}{B_c T_c} \mathbf{E} \left[\log \left(1 + \frac{P g_{\min} \psi}{\delta N_t N_0 B} B_c T_c \right) \right],
\end{aligned} \tag{44}$$

Equation (a) is due to $g_{\min} = \min_{m,u,v} \mathbf{E} [|h[m]^{(u,v)}|^2]$ is the minimum element in the diagonals of $\Lambda^{(v)}$ and among all v 's, and (b) stems from the relation between determinant and eigenvalues. Since Ξ is a $K \times MN_t$ circulant matrix containing the power normalized vector \mathbf{x}/\sqrt{P} in its first column, the n -th eigenvalue of $\Xi^\dagger \Xi$ is given by

$$\lambda_n(\Xi^\dagger \Xi) = \left| \sum_{k=0}^{K-1} \frac{\mathbf{x}_k}{\sqrt{P}} e^{-j2\pi \frac{kn}{MN_t}} \right|^2 \triangleq K \psi_{K,n}, \quad n = 1, \dots, MN_t.$$

Since $\mathbb{E}[\psi_{K,n}] \leq \frac{1}{KP} |\sum_{k=0}^{K-1} \mathbf{x}_k|^2 \leq 1$ owing to the power constraint $\mathbb{E}[\mathbf{x}] \leq P$, we obtain (c) by the fact that $B_c T_c < K$ and by the definition of ψ in (12). Moreover, we have $\psi > 0$ because the rate penalty of non-peaky inputs in active cycles is non-zero ($\delta \mathbf{I}(\mathbf{H}; \mathbf{y} | \tilde{\mathbf{x}} / \sqrt{\delta}) > 0$).

APPENDIX G

PROOF OF LEMMA 4

We define $(\delta B)^\pm$ such that

$$\frac{P}{(\delta B)^\pm N_0} = \sqrt{\Omega \frac{\log(B_c T_c)}{B_c T_c}} + o\left(\sqrt{\frac{\log(B_c T_c)}{B_c T_c}}\right). \quad (45)$$

Substituting (45) into (11) we obtain that

$$R^{UB}(\delta B) = \frac{P N_r}{N_0} \left[1 - \frac{1}{2} \sqrt{\Omega \frac{\log(B_c T_c)}{B_c T_c}} - N_t \frac{\mathbb{E} \left[\log(1 + \sqrt{\Omega B_c T_c \log(B_c T_c)} g_{\min} \psi / N_t) \right]}{\sqrt{\Omega B_c T_c \log(B_c T_c)}} \right] + o\left(\sqrt{\frac{\log(B_c T_c)}{B_c T_c}}\right). \quad (46)$$

We separate the logarithm in two parts

$$R^{UB}(\delta B) = \frac{P N_r}{N_0} \left[1 - \frac{1}{2} \sqrt{\Omega \frac{\log(B_c T_c)}{B_c T_c}} - \frac{1}{2} \frac{N_t \log(B_c T_c)}{\sqrt{\Omega B_c T_c \log(B_c T_c)}} - N_t \frac{\mathbb{E} \left[\log\left(\frac{1}{\sqrt{B_c T_c}} + \sqrt{\Omega \log(B_c T_c)} g_{\min} \psi / N_t\right) \right]}{\sqrt{\Omega B_c T_c \log(B_c T_c)}} \right] + o\left(\sqrt{\frac{\log(B_c T_c)}{B_c T_c}}\right). \quad (47)$$

Since $\mathbb{E}[\psi] \leq 1$, the third negative part is also $o\left(\sqrt{\frac{\log(B_c T_c)}{B_c T_c}}\right)$. We have

$$R^{UB}(\delta B) = \frac{P N_r}{N_0} \left[1 - \sqrt{\frac{\log(B_c T_c)}{B_c T_c}} \frac{1}{2} \left(\sqrt{\Omega} + \frac{N_t}{\sqrt{\Omega}} \right) \right] + o\left(\sqrt{\frac{\log(B_c T_c)}{B_c T_c}}\right). \quad (48)$$

We will make this upper bound equal the achievable value in (10), which leads to

$$\frac{1}{2} \left(\sqrt{\Omega} + \frac{N_t}{\sqrt{\Omega}} \right) = \sqrt{(\kappa - 2 + N_t + N_r) \log \pi} + o\left(\sqrt{\frac{B_c T_c}{\log(B_c T_c)}}\right). \quad (49)$$

By making change of variable $\Upsilon = \Omega / N_t$ we get

$$\left(\sqrt{\Upsilon} + \frac{1}{\sqrt{\Upsilon}} \right) = 2 \sqrt{\left(\frac{\kappa - 2 + N_r}{N_t} + 1 \right) \log \pi} + o\left(\sqrt{\frac{B_c T_c}{\log(B_c T_c)}}\right). \quad (50)$$

With $\kappa = 2$ for Rayleigh fading, $(\frac{\kappa-2+N_r}{N_t} + 1) \geq 1$. We obtain the following two roots of (50)

$$\begin{aligned}\sqrt{\Upsilon}^- &= \sqrt{(\frac{N_r}{N_t} + 1) \log \pi} + \sqrt{(\frac{N_r}{N_t} + 1) \log \pi - 1} + o(\sqrt{\frac{B_c T_c}{\log(B_c T_c)}}), \\ \sqrt{\Upsilon}^+ &= \sqrt{(\frac{N_r}{N_t} + 1) \log \pi} - \sqrt{(\frac{N_r}{N_t} + 1) \log \pi - 1} + o(\sqrt{\frac{B_c T_c}{\log(B_c T_c)}}).\end{aligned}\tag{51}$$

It is ready to see that

$$\begin{aligned}\sqrt{\Omega}^- &= \sqrt{N_t} \sqrt{\Upsilon}^- \leq 2\sqrt{(N_r + N_t) \log \pi} + o(\sqrt{\frac{B_c T_c}{\log(B_c T_c)}}), \\ \sqrt{\Omega}^+ &= \sqrt{N_t} \sqrt{\Upsilon}^+ \geq \frac{N_t}{2\sqrt{(N_r + N_t) \log \pi}} + o(\sqrt{\frac{B_c T_c}{\log(B_c T_c)}}).\end{aligned}\tag{52}$$

Substituting them back in (45) we get the points $(\delta B)^-$ and $(\delta B)^+$ as shown in (14). Therefore the true achievement of the maximum can only occur in the range $(\delta B)_{\text{crit}} \in [(\delta B)^-, (\delta B)^+]$.

ACKNOWLEDGMENT

We would like to thank the anonymous reviewers and the editor for all the helpful comments. We also thank Dr. Wenyi Zhang for helpful discussion on an earlier version of this paper.

REFERENCES

- [1] F. Gómez-Cuba, J. Du, M. Médard, and E. Erkip, “Bandwidth Occupancy of Non-Coherent Wideband Fading Channels,” in *IEEE International Symposium on Information Theory (ISIT)*, 2015.
- [2] Z. Pi and F. Khan, “An Introduction to Millimeter-Wave Mobile Broadband Systems,” *IEEE Communications Magazine*, vol. 49, pp. 101–107, Jun. 2011.
- [3] P. Pietraski, D. Britz, A. Roy, R. Pragada, and G. Charlton, “Millimeter Wave and Terahertz Communications: Feasibility and Challenges,” *ZTE Communications*, vol. 10, no. 4, pp. 3–12, 2012.
- [4] S. Rangan, T. T. S. Rappaport, and E. Erkip, “Millimeter-Wave Cellular Wireless Networks: Potentials and Challenges,” *Proceedings of the IEEE*, vol. 102, no. 3, pp. 366–385, Mar. 2014.
- [5] T. S. Rappaport, R. W. Heath Jr., R. C. Daniels, and J. N. Murdock, *Millimeter Wave Wireless Communications*. Pearson Education, 2014.
- [6] M. Médard and R. G. Gallager, “Bandwidth Scaling for Fading Multipath Channels,” *IEEE Transactions on Information Theory*, vol. 48, pp. 840–852, Apr. 2002.
- [7] A. Lozano and D. Porrat, “Non-Peaky Signals in Wideband Fading Channels: Achievable Bit Rates and Optimal Bandwidth,” *IEEE Transactions on Wireless Communications*, vol. 11, pp. 246–257, Jan. 2012.
- [8] L. Zheng, D. N. C. Tse, and M. Medard, “Channel Coherence in the Low-SNR Regime,” *IEEE Transactions on Information Theory*, vol. 53, pp. 976–997, Mar. 2007.
- [9] S. Ray, M. Medard, and L. Zheng, “On Noncoherent MIMO Channels in the Wideband Regime: Capacity and Reliability,” *IEEE Transactions on Information Theory*, vol. 53, pp. 1983–2009, Jun. 2007.

- [10] V. Subramanian and B. Hajek, "Broad-band Fading Channels: Signal Burstiness and Capacity," *IEEE Transactions on Information Theory*, vol. 48, pp. 809–827, Apr. 2002.
- [11] B. Hajek and V. Subramanian, "Capacity and Reliability Function for Small Peak Signal Constraints," *IEEE Transactions on Information Theory*, vol. 48, pp. 828–839, Apr. 2002.
- [12] I. E. Telatar and D. N. Tse, "Capacity and Mutual Information of Wideband Multipath Fading Channels," *IEEE Transactions on Information Theory*, vol. 46, pp. 1384–1400, Jul. 2000.
- [13] S. Verdú, "Spectral Efficiency in the Wideband Regime," *IEEE Transactions on Information Theory*, vol. 48, pp. 1319–1343, Jun. 2002.
- [14] C. Luo, M. Medard, and L. Zheng, "On Approaching Wideband Capacity Using Multitone FSK," *IEEE Journal on Selected Areas in Communications*, vol. 23, no. 9, pp. 1830–1838, Sep. 2005.
- [15] W. Zhang and J. N. Laneman, "How Good Is PSK for Peak-Limited Fading Channels in the Low-SNR Regime?" *IEEE Transactions on Information Theory*, vol. 53, pp. 236–251, Jan. 2007.
- [16] V. Sethuraman, L. Wang, B. Hajek, and A. Lapidoth, "Low-SNR Capacity of Noncoherent Fading Channels," *IEEE Transactions on Information Theory*, vol. 55, pp. 1555–1574, Apr. 2009.
- [17] G. Durisi, U. Schuster, H. Bolcskei, and S. Shamai, "Noncoherent Capacity of Underspread Fading Channels," *IEEE Transactions on Information Theory*, vol. 56, pp. 367–395, Jan. 2010.
- [18] U. Schuster, G. Durisi, H. Bolcskei, and H. Poor, "Capacity bounds for peak-constrained multiantenna wideband channels," *IEEE Transactions on Communications*, vol. 57, pp. 2686–2696, Sep. 2009.
- [19] V. Sethuraman and B. Hajek, "Capacity Per Unit Energy of Fading Channels With a Peak Constraint," *IEEE Transactions on Information Theory*, vol. 51, pp. 3102–3120, Sep. 2005.
- [20] H. Artes, G. Matz, and F. Hlawatsch, "Unbiased Scattering Function Estimators for Underspread Channels and Extension to Data-Driven Operation," *IEEE Transactions on Signal Processing*, vol. 52, no. 5, pp. 1387–1402, May 2004.
- [21] G. Durisi, V. Morgenshtern, and H. Bolcskei, "On the Sensitivity of Continuous-Time Noncoherent Fading Channel Capacity," *IEEE Transactions on Information Theory*, vol. 58, pp. 6372–6391, Oct. 2012.
- [22] N. Jindal and A. Lozano, "A Unified Treatment of Optimum Pilot Overhead in Multipath Fading Channels," *IEEE Transactions on Communications*, vol. 58, pp. 2939–2948, Oct. 2010.
- [23] A. Lapidoth, "On the asymptotic capacity of stationary Gaussian fading channels," *IEEE Transactions on Information Theory*, vol. 51, pp. 437–446, Feb. 2005.
- [24] T. S. Rappaport, S. Sun, R. Mayzus, H. Zhao, Y. Azar, K. Wang, G. N. Wong, J. K. Schulz, M. M. Samimi, and F. Gutierrez, "Millimeter Wave Mobile Communications for 5G Cellular: It Will Work!" *IEEE Access*, vol. 1, pp. 335–349, May 2013.
- [25] Z. Zhang, J. Ryu, S. Subramanian, and A. Sampath, "Coverage and Channel Characteristics of Millimeter Wave Band Using Ray Tracing," in *IEEE International Conference on Communications (ICC)*, Jun. 2015, pp. 1380–1385.
- [26] M. R. Akdeniz, Y. Liu, M. K. Samimi, S. Sun, S. Rangan, T. S. Rappaport, E. Erkip, and S. Member, "Millimeter Wave Channel Modeling and Cellular Capacity Evaluation," *IEEE Journal on Selected Areas in Communications*, vol. 32, pp. 1164–1179, Apr. 2013.